Biophysical Chemistry 5 (1976) 207–241

MOLECULAR WEIGHTS AND MOLECULAR-WEIGHT DISTRIBUTIONS FROM ULTRACENTRIFUGATION OF NONIDEAL SOLUTIONS

Peter J. WAN* and E.T. ADAMS, Jr.**
Chemistry Department, Texas A&M University, College Station, Texas 77843, USA

Ultracentrifugation, membrane osmometry and capillary viscometry experiments have been performed on two dextran samples, which have molecular-weight distributions (MWDs) similar to those of dextrans used as blood plasma extenders. The manufacturer reported values of M_n and M_w, determined by end group analysis and by light scattering, respectively. Our values of M_n, determined by osmometry, and M_w, calculated from ultracentrifugal and viscometry experiments, agreed quite well with the manufacturer's results. Good agreement was obtained with values of M_w and B_{LS} (the light scattering second virial coefficient) obtained from sedimentation equilibrium experiments at different speeds using sector or nonsector-shaped centerpieces. Several ways of obtaining M_w, M_z and B_{LS} from sedimentation equilibrium experiments are presented. We have also shown how to obtain the speed-dependent term of the sedimentation equilibrium second virial coefficient.

Both B_{LS} and the speed-dependent nonideal terms could be used to correct the sedimentation equilibrium data, so that ideal values of $d \ln c/d(r^2)$ or $dc/d(r^2)$ could be estimated and used to obtain the MWDs of the dextran samples. Both Donnelly's and Scholte's methods were used with the sedimentation equilibrium data. With both methods, unimodal MWDs were encountered, which gave good agreement with the manufacturer's MWDs, obtained by a combination of analytical gel chromatography and light scattering. Uncorrected sedimentation equilibrium data gave MWDs quite different from the manufacturer's results. The MWD calculated from the differential distribution of sedimentation coefficients also gave a unimodal MWD, but this MWD did not give as good agreement with the sedimentation equilibrium results or with the manufacturer's results.

1. Introduction

The ultracentrifuge was introduced to macromolecular chemists in 1924 by Svedberg and Rinde [2]. Four years later Rinde [3] developed methods for obtaining a distribution of radii of colloidal gold sols from sedimentation equilibrium experiments. Subsequent methods for obtaining molecular-weight distributions (MWDs) of polymeric solutes from sedimentation equilibrium experiments were largely based on Rinde's pioneering work [4a,5,6a,7]. In 1935 Lansing and Kraemer [8] in their historic paper pointed out the existence of various average molecular weights, and they showed how one might obtain the weight (M_w) and z (M_z) average molecular weights from sedimentation equilibrium experiments in ideal dilute solutions.

Early attempts to evaluate M_w or M_z of polymeric solutes under nonideal solution conditions were not too successful, since the redistribution of the polymeric solutes in the centrifugal field produced an added complication which is not encountered in light scattering or osmotic pressure experiments [5,6b,7–14]. This adverse situation tended to put a pall on studies of polydisperse macromolecules by sedimentation equilibrium experiments [14]. The way out of this dilemma was indicated by the theories of Fujita [15,16] and of Osterhoudt and Williams [17]. Tney have shown how

* This paper is based in part on the dissertation submitted by Peter J. Wan to the Graduate College of Texas A&M University in partial fulfillment of the requirements for the degree of Doctor of Philosophy (December 1973). Present Address: Oil Seed Products Division, Texas Engineering Experiment Station, F.E. Box 183, College Station, Tx 77843.

** Please address all correspondence regarding this paper to Dr. E.T. Adams, Jr., Chemistry Department, Texas A&M University, College Station, Texas 77843. Part of this material was presented before the Division of Polymer Chemistry at the 167th National Meeting of the American Chemical Society in Los Angeles, California, March 30–April 5, 1974 [1].

one may evaluate M_w under nonideal solution conditions. Experimental tests of these theories have been reported with narrow MWD polymers [18] or with a blend of two "monodisperse" polymers [19]. In both cases linear polymers were used.

Until quite recently most of the methods for obtaining MWDs of polymers from sedimentation equilibrium experiments had two requirements: ultracentrifuge cells having sector-shaped centerpieces had to be used, and ideal, dilute solution (theta) conditions had to prevail. We have shown [7] how both of these restrictions can be removed, and in this paper we present a test of our ideas. In order to obtain the MWDs it is necessary to obtain values of the M_w and M_z of the samples, as well as the light scattering second virial coefficient, B_{LS}, and other nonideal terms from sedimentation equilibrium experiments. These will be reported and dealt with in section three of this paper. In addition we will report values of M_n, the number average molecular weight, which was determined by membrane osmometry, as well as values of $[\eta]$, the intrinsic viscosity. The value of s_w, the weight average sedimentation coefficient, has been determined for one of the samples. We will report on values of M_w calculated from $[\eta]$ or from s_w. Since the manufacturer (Pharmacia Fine Chemicals) has also measured M_w (by light scattering) and M_n (by end-group analysis) of the dextran samples [20], these experiments give us an opportunity to compare the results obtained by different physical techniques on the same materials. The dextran samples used in these experiments are similar in molecular weight range to clinical dextrans which are used as blood plasma extenders and for the treatment of shock [21–23]. Furthermore, the dextrans are slightly branched and have a broader MWD than the materials used by Albright and Williams [18] or by Utiyama, Tagata and Kurata [19]. We will also show that the method advocated by Albright and Williams [18] for obtaining M_w and B_{LS} can be extended to cells having nonsector-shaped centerpieces. A method for obtaining the speed-dependence of the sedimentation equilibrium second virial coefficient will be shown.

In section four of this paper we will report on the MWDs of the two dextran samples. First we show how the nonideal terms obtained in the section three can be applied to the basic sedimentation equilibrium equation so that the ideal concentration or concentration gradient distributions can be estimated. Once this is done, one could use any of the methods that have been reported for obtaining MWDs from sedimentation equilibrium experiments [12,24–36]. We have chosen to illustrate our procedure with Donnelly's [24,25] and with Scholte's [26–28] methods. Results obtained with sector- or nonsector-shaped centerpieces will be reported. Sedimentation velocity experiments can also be used to obtain MWDs from values of $g^0(s_0)$, the differential distribution of sedimentation coefficients [5,6c,23,37,38]; here we report on the MWD of one of the samples using data obtained from sedimentation velocity experiments in addition to the MWD obtained by sedimentation equilibrium experiments. We will compare the MWDs obtained by ultracentrifugal methods with those reported by the manufacturer (Pharmacia Fine Chemicals) on these dextran samples.

2. Materials and methods

2.1. Dextran solutions

The dextran samples used in this work were T-70 type dextrans, obtained from Pharmacia Fine Chemicals. Two different lots were used in these studies. For each lot the manufacturer provided information sheets which had plots of the differential and integral MWD; their MWDs were determined by analytical gel chromatography and by light scattering [20,39,40]. In addition these information sheets gave values of $[\eta]$, the intrinsic viscosity, in aqueous solutions at 20°C, and also the weight (M_w) and number (M_n) average molecular weights. Table 1 summarizes the data provided by the manufacturer. Stock solutions of the dextrans (approximately 15 g/ℓ) were prepared by dissolving the dextrans in boiled, double distilled water. Other solutions were prepared by weight dilution of the stock solutions. When not in use, the dextran solutions were kept frozen. Intrinsic viscosity measurements on fresh and on thawed, stored solutions gave the same result, which suggests that freezing did not degrade the samples.

2.2. Concentration determination and partial specific volume

Concentrations of the dextran solutions were determined by differential refractometry (Brice Phoenix Dif-

Table 1
Manufacturer's values of $[\eta]$, M_n and M_w for the dextran samples

Batch No.	$[\eta]$ a) (dl/g)	M_n b) (dalton)	M_w c) (dalton)
7981	0.26	41000	67500
683	0.26	39500	69500

a) Determined by capillary viscometry of aqueous solutions at 20°C.
b) Determined by end group analyses.
c) Determined by light scattering.

ferential Refractometer); the instrument was thermostatted at 25°C. The differential refractometer was calibrated with KCl solutions using the data of Kruis [41]. All measurements on the differential refractometer were carried out at a wavelength (λ) of 546 nm, the wavelength of visible light ordinarily used in the ultracentrifuge. At λ = 546 nm, the refractive index increment, $(\partial n/\partial c)_{T,P}$, was taken to be 1.50×10^{-4} ℓ/g [42a], which was the average of several measurements of the refractive index increment.

Since the ultracentrifuges used in these experiments were equipped for Rayleigh and schlieren optics, the total solute concentrations, c, were expressed as fringes, J. The number of fringes, J, is related to the refractive index difference, $n - n_0$, between the solution and the solvent, by [13,43,44]

$$J = h(n - n_0)/\lambda. \tag{1}$$

Several thicknesses of centerpieces, h, are available, but the most common size is a 12 mm centerpiece, so all fringe concentrations are based on this size centerpiece. Since

$$n - n_0 = (\partial n/\partial c)_{T,P} c, \tag{2}$$

J is related to c by

$$J = h(\partial n/\partial c)_{T,P} c/\lambda. \tag{3}$$

At 25°C with λ = 546 nm and $(\partial n/\partial c)_{T,P} = 1.50 \times 10^{-4}$ ℓ/g, one obtains (for c in g/ℓ)

$$J = 3.29_7 c. \tag{4}$$

Some experiments were performed with an ultracentrifuge equipped with a helium-neon laser as an additional light source. The fringes produced by the red laser light (λ = 632.8 nm) can be related to the fringes produced by the green light (λ = 546 nm) isolated from the mercury vapor lamp. To do this one chooses two radial positions, r_1 and r_2, in the solution column of the ultracentrifuge cell and counts the number of fringes produced between the two radial positions by each light source. Doing this the following relation was obtained:

$$J(632.8\text{ nm}) = 0.8765\, J(546\text{ nm}). \tag{5}$$

This equation was used to convert the red fringes to the equivalent number of green fringes.

Density measurements were graciously done for us Dr. David Cox at the University of Texas in Austin. These measurements were carried out at 19.8°C on a digital, precision density meter (Anton Paar Model DMA 02C). The quantities $\bar{v}$ and $(1 - \bar{v}\rho_0)$ were calculated from the slope of a plot of ρ vs c, since [45]

$$\rho = \rho_0 + (1 - \bar{v}\rho_0)(c/1000). \tag{6}$$

Here ρ_0 is the solvent density. From these measurements we obtained $(1 - \bar{v}\rho_0) = 0.407_6$ and $\bar{v}$ = 0.593 ml/g. The Polymer Handbook reports a value of $\bar{v}$ = 0.6 ml/g at 20.9°C for aqueous dextran solutions [42b].

2.3. Intrinsic viscosity ($[\eta]$)

Measurements of $[\eta]$ were done by capillary viscometry (Cannon–Ubbelohde 50) in a thermostatted water bath at 20 ± 0.02°C. All stock solutions and distilled water were filtered through a millipore filter (0.45 μ pore size). Successive dilutions of the stock solutions were made by adding a definite amount of distilled water the viscometer. The intrinsic viscosity was calculated from the relative viscosity, η_r, by the relation [46a,47]

$$\lim_{c \to 0} (\ln \eta_r)/c = [\eta] \tag{7}$$

or from the specific viscosity, η_{sp}, since [46a,47]

$$\lim_{c \to 0} \eta_{sp}/c = [\eta]. \tag{8}$$

2.4. Membrane osmometry

The osmotic pressure measurements of the dextran

solutions at several different temperatures were carried out in a high speed, membrane osmometer (Melabs Model CSM-2) using cellulose membranes. The membranes (Schleicher and Schuell B19 membranes) were conditioned by soaking in distilled water for at least 12 hours before use. Values of M_n, the number average molecular weight, and B_{OS}, the osmotic pressure second virial coefficient, were obtained from plots of $1000\pi/c$ vs c (in g/ℓ), since [46b, 48]

$$\frac{1000\pi}{c} = \frac{RT}{M_{na}} = RT\left(\frac{1}{M_n} + B_{OS}c\right). \quad (9)$$

Here π is the osmotic pressure, R is the gas constant, T is the absolute temperature and M_{na} is the apparent number average molecular weight. Plots of $1000\pi/c$ vs c for one dextran sample at various temperatures are shown in fig. 1.

2.5. Ultracentrifugation

The ultracentrilfuge experiments reported here were carried out at 20 ± 0.1°C for the sedimentation velocity experiments and at 25 ± 0.1°C for the sedimentation equilibrium experiments on ultracentifuges equipped for Rayleigh and schlieren optics.

Both ultracentrifuges had electronic speed controls; rotor temperature (± 0.1°C) was obtained from the RTIC (resistance temperature indicator and control) unit. Most of the Rayleigh and schlieren data were obtained at 546 nm (the green line of mercury) and photographed on Kodak Metallographic or Type II G plates. The photographic patterns were read on a comparator (Nikon Model 6C). Some experiments were also performed on a second ultracentrifuge which had been modified so that a modulatable, helium-neon laser could also be used as a light source. The photographic data on this ultracentrifuge were recorded on Type IV F, 70 mm, spectroscopic film which has a polyester base.

Sedimentation velocity experiments were carried out at 60000 RPM. Since most double sector centerpieces tended to leak at this speed, these experiments were performed in two single sector cells — one cell containing the solution and the other containing water to give a baseline; the side index on the rotor was used as a distance reference. Only schlieren optics could be used in this case.

Sedimentation equilibrium experiments were performed in two kinds of cells. One cell had double sector

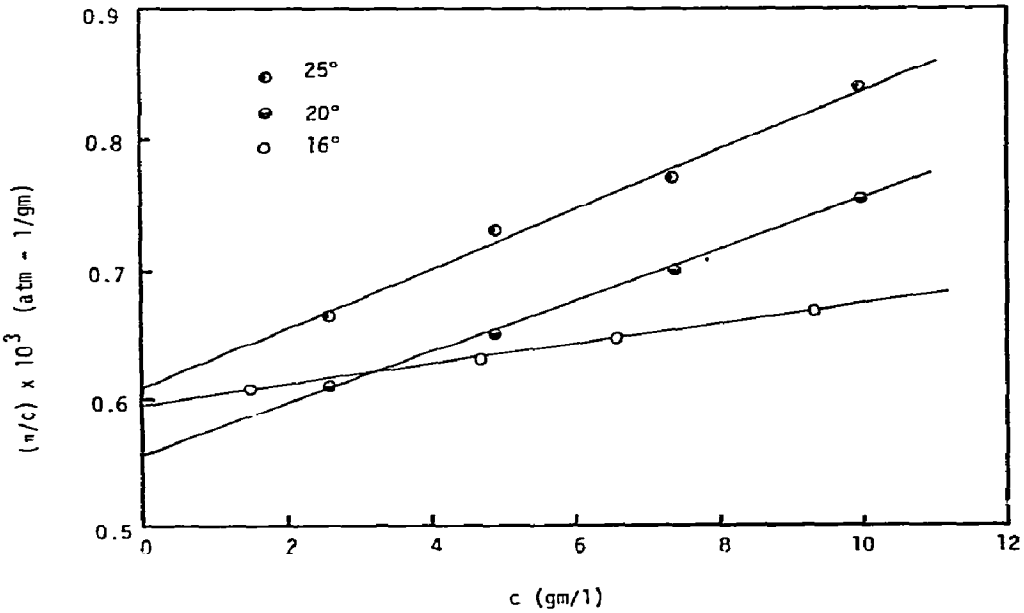

Fig. 1. High speed membrane osmometry at various temperatures. Plots of $1000\pi/c$ vs c [see eq. (9)] for lot 693 are displayed here. From the intercept of these plots we can obtain M_n, and from the limiting slope we can get B_{OS}.

centerpieces; the other cell had a six-hole multichannel equilibrium centerpiece [49]. One side of each centerpiece was reserved for the solvent, and the other side was reserved for the solution or solutions. In multichannel equilibrium centerpieces, the most concentrated solution is placed in the innermost hole and the most dilute solution is placed in the outermost hole. The cell filling procedure advocated by Adams and Lewis [50] was scrupulously followed. No layering oils were used. The radial position of the cell bottom, r_b, was determined from careful measurements of the centerpiece and the assembled cell on the comparator; it was also checked by using a weighed amount of water, whose volume can be calculated from the density at the appropriate temperature, in the cell and photographing the schlieren pattern at the operating speed. Since the volume of water, r_m, the cell thickness and the sector angle are known, r_b can be calculated. The time to reach sedimentation equilibrium was estimated using the method of Van Holde and Baldwin [51]; the diffusion coefficient needed for this estimate was estimated from values tabulated for dextran solutions in the Polymer Handbook [42b]. Photographs were taken shortly after the rotor reached the desired speed and at least six hours later than the time estimated to reach sedimentation equilibrium. Four or more rotor speeds (from 4400 to 34000 RPM) were used for each solution; successive rotor speeds were separated roughly by a factor of $\sqrt{2}$. The sequence of speeds was to start at the lowest desired speed, obtain sedimentation equilibrium at that speed, record the Rayleigh and schlieren patterns, and then proceed to the next higher speed. This sequence of events was reported for each successive speed.

3. Average molecular weights and other physical properties of the dextrans

The results of the various experiments are summarized in table 2 and are discussed individually below. Table 2 is organized so that the average molecular weights are listed first. The next grouping of the data includes the second virial coefficients and other nonideal terms, and the final group of data includes other quantities such as $[\eta]$, s_w and $\bar{v}$.

3.1. Intrinsic viscosity

The intrinsic viscosity, $[\eta]$, was determined from the intercepts of the least squares straight line drawn through plots of $\ln \eta_r/c$ vs c [see eq. (7)] or from plots of η_{sp}/c vs c [see eq. (8)]. For batch 7981 a value of $[\eta] = 0.259$ dl/g was obtained at 20°C using eq. (8); with eq. (7) the value of $[\eta] = 0.260$ dl/g was obtained. The average value of these measurements was $[\eta] = 0.260 \pm 0.001$ dl/g. Using the same procedures with batch number 693 we obtained an average value of $[\eta] = 0.260 \pm 0.001$ dl/g. The Mark–Houwink [39,46a] equation,

$$[\eta] = KM_w^{\alpha}, \tag{10}$$

was used to estimate M_w. The constants, $K = 2.43 \times 10^{-3}$ dl/g and $\alpha = 0.42$, were taken from Granath's paper [39]; Granath has studied the MWD and other physical properties of some Pharmacia dextrans, including some prepared from the same strain of *Leuconostoc mesenteroides* used to produce our samples. From these values of K and α, a value of $M_w = 6.79 \times 10^4$ dalton was obtained for both batches.

3.2. Osmotic pressure

Osmotic pressure experiments were performed at various temperatures in an attempt to find ideal, dilute solution conditions, but as fig. 1 shows this was not the case. The values of M_n, the number average molecular weights and B_{OS}, the osmotic pressure second virial coefficients at the various temperatures, are listed in table 3. Table 2 list the average of the M_n values.

3.3. Sedimentation velocity experiments

These experiments were performed only with the dextran from Batch No. 7981. Since the solute sedimented very slowly, the apparent weight average sedimentation coefficients, s_{wa}, at various concentrations were calculated using the method of Webber [52]. The quantity $\overline{r^2}$, which is the square of the radial position of the second moment of the moving boundary curve, is given by

$$\overline{r^2} = (1/c_p)\left(c_m r_m^2 + \int_{r_m}^{r_p} r^2 (dc/dr)\, dr\right). \tag{11}$$

Table 2
Some physical properties of the dextran T-70 samples $t = 25°C$ (unless otherwise indicated)

Property	Units	Lot 7981	Lot 693	Method used
$M_n \times 10^{-4}$	dalton	4.30	4.08	Membrane osmometry
$M_w \times 10^{-4}$	dalton	6.58	6.81	Sedimentation equilibrium [a]
$M_w \times 10^{-4}$	dalton	6.64	6.85	Sedimentation equilibrium [b]
$M_w \times 10^{-4}$	dalton	6.79	6.79	Intrinsic viscosity
$M_w \times 10^{-4}$	dalton	6.64	–	Sedimentation velocity (s_w)
$M_z \times 10^{-4}$	dalton	11.5	11.6	Sedimentation equilibrium
$B_{LS} \times 10^6$	mole/(g) (fringe) mole ℓ/g^2	0.322 1.06	0.296 0.974	Sedimentation equilibrium [a]
$B_{LS} \times 10^6$	mole/(g) (fringe) mole ℓ/g^2	0.323 1.06	0.304 1.00	Sedimentation equilibrium [b]
$B_{OS} \times 10^6$	mole ℓ/g^2	0.354 (20°C)	0.934 (25°C)	Membrane osmometry
$B_{SZ} \times 10^6$	mole/(g) (fringe) mole ℓ/g^2	0.250 0.820	0.217 0.712	Sedimentation equilibrium
α	g/(mole) (fringe) ℓ/mole	22.8 74.8	15.2 49.9	Sedimentation equilibrium
β	g/(mole) (fringe) ℓ/mole	– –	5.02 16.5	Sedimentation equilibrium
$[\eta]$	dl/g	0.26	0.26	Capillary viscometry at 20°C
s_w	svedberg	3.70	–	Sedimentation velocity at 20°C (second moment)
$\bar{v}$	ml/g	0.593	–	Precision density measurements at 19.8°C

[a] Calculated using the Albright and Williams [18] method of experiments at different speeds.
[b] Calculated from experiments at different speeds using a modification of a method proposed by Fujita [15].

Table 3
Values of M_n and B_{OS} at various temperatures

Lot number	t (°C)	$M_n \times 10^{-4}$ (dalton)	$B_{OS} \times 10^6$ (mole ℓ)/g^2
7981	20	4.30	0.354
693	16	3.98	0.326
	20.1	4.24	0.713
	25	4.01	0.934
	Average M_n (4.08 ± 0.11) × 10^4 for Lot 693		

Here c_m is the concentration of solute at the air-solution meniscus, whose radial position is r_m; c_p is the solute concentration in the plateau region, the region in which the concentration gradient, dc/dr, is zero. The quantity r_p is the radial position in the solution column of the ultracentrifuge cell at which the plateau begins, and r is any radial position between r_m and r_p. In order to evaluate $\bar{r^2}$, one has to know c_0, the initial concentration, and the value of c_m, which is calculated from the equation [53]

$$c_m = c_0 - (1/r_m^2) \int_{r_m}^{r_p} r^2 (dc/dr)\, dr. \qquad (12)$$

In addition one must know c_p, which is obtained from

$$c_p = c_m + \int_{r_m}^{r_p} (dc/dr)\, dr. \qquad (13)$$

Values of $\bar{r}^2$ are calculated at various times, t, and the s_{wa} are obtained from the slopes of plots of $\ln \bar{r}$ vs t, since [5,45]

$$\ln \bar{r} = s_{wa}\omega^2 t. \tag{14}$$

Zero time corrections were applied using the method proposed by Elias [54]. The values of $1/s_{wa}$ obtained for each solution are plotted against c_{av} to obtain the weight average sedimentation coefficient, s_w, from the intercept, which gives $1/s_w$. Here we used the equation [45]

$$1/s_{wa} = (1/s_w) + k_s c_{av}. \tag{15}$$

The quantity k_s is a sedimentation coefficient concentration dependence parameter; the quantity c_{av} is calculated as follows:

$$c_{av} = c_0(r_m^2/\bar{r}_{av}^2), \tag{16}$$

where $\bar{r}_{av}^2$ represents the average values of $\bar{r}^2$; it is estimated by dividing the sum of the values of r^2 for the first and the last pictures used by 2. Fig. 2 shows the plot of $1/s_{wa}$ *vs* c_{av}; here we obtained $s_w = 3.72$ S at 20°C in water. Using an equation analogous to the Mark–Houwink equation, namely, [39,45]

$$s = KM_w^{\alpha} \tag{17}$$

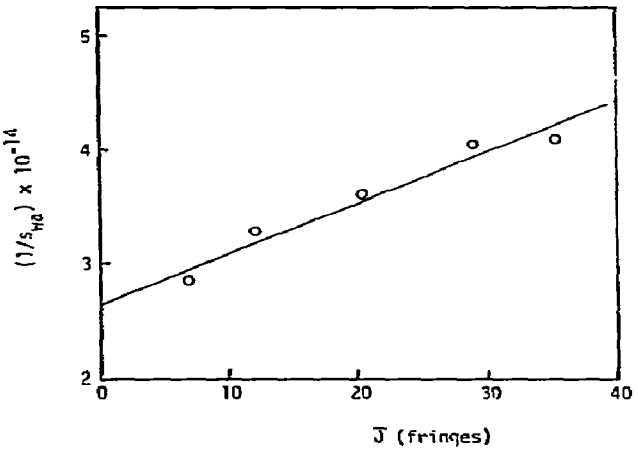

Fig. 2. Sedimentation velocity experiments. Plots of $1/s_{wa}$ vs c_{av} for lot 7981 are shown here; the experiments were performed at 20°C. The intercept of these plots gives $1/s_w$ [see eq. (15)]. From the slope of this plot we obtained $k_s = 4.185 \times 10^{10}$ g s^{-1} gm^{-1}.

we obtained $M_w = 6.69 \times 10^4$ dalton. The values of K and α used here were $K = 2.24 \times 10^{-15}$ s and $\alpha = 0.46$; these quantities were calculated from the values of s_0 and M_w reported by Granath [39].

3.4. Sedimentation equilibrium experiments

We will use the basic sedimentation equilibrium equation (see appendix A.1) for the correction of nonideal behavior. In order to apply the nonideal corrections, it is necessary to obtain the M_w, M_z, B_{LS} and other nonideal properties of the polymeric sample. To do this it is necessary to use average or apparent average molecular weights over the cell. Conservation of mass equations (see refs. [4b,5,6d and 7] for more details) are necessary for the evaluation of the concentration at any radial position r ($r_m \leq r \leq r_b$) in the ultracentrifuge cell whenever Rayleigh or schlieren optics are used. The solute concentration, $c = c_r$, at any radial position r must be known in order to evaluate $M_{w\ \text{cell}}$ or $M_{w\ \text{cell app}}$. The conservation of mass equations used depend on the volume of the centerpiece, which in turn depends on the shape of the centerpiece used. The equation used for the evaluation of $M_{z\ \text{cell}}$ or $M_{z\ \text{cell app}}$ also depends on the type of centerpiece used. Thus, at this point we will have to use equations that are appropriate for the particular type of centerpiece being used.

3.4.1. Sector-shaped centerpieces

For sector-shaped centerpieces $M_{w\ \text{cell app}}$, the apparent weight average molecular weight over the cell is defined by the familiar equation [4a,5,6a,7,13,15–19]

$$\Delta c/c_0 = \Delta J/J_0 = \Lambda M_{w\ \text{cell app}}, \tag{18}$$

where

$$\Lambda = (1 - \bar{v}\rho_0)\,\omega^2\,(r_b^2 - r_m^2)/2RT, \tag{19}$$

$$\Delta c = c_b - c_m, \tag{20}$$

and

$$\Delta J = J_b - J_m. \tag{21}$$

The quantity Δc is the change in the solute concentration between r_m and r_b, the radial position of the cell bottom. This concentration change can also be expressed in fringe notation as ΔJ. Because of eq. (3), $\Delta c/c_0$

$= \Delta J/J_0$; here c_0 (or J_0) is the initial solute concentration. The quantities making up Λ have their usual meaning: ω is the angular velocity of the rotor [$\omega = 2\pi(\text{RPM})/60$]; R is the gas constant; T is the absolute temperature; the other quantities making up Λ have already been defined. For ideal, dilute solutions $M_{\text{w cell app}}$ is the M_w of the polymeric solute.

Another average over the cell is the quantity $M_{\text{w cell vol app}}$, which is defined by [4a,7,8,55]

$$\ln c_b/c_m = \ln J_b/J_m = M_{\text{w cell vol app}}. \quad (22)$$

It has been shown [55] for ideal, dilute solutions that $M_{\text{w cell}} > M_{\text{w cell vol}}$ at real speeds; the same arguments can be used to show that at real speeds $M_{\text{w cell app}} > M_{\text{w cell vol app}}$. For experiments at several speeds, it has been shown that [7,17,18]

$$\lim_{\Lambda\to 0} M_{\text{w cell app}} = \lim_{\Lambda\to 0} M_{\text{w cell vol app}} = M^0_{\text{w app}}, \quad (23)$$

where $M^0_{\text{w app}}$ is defined by [7,17,18]

$$M^0_{\text{w app}} = M_w(1 - B_{LS}c_0M_w - \ldots), \quad (24)$$

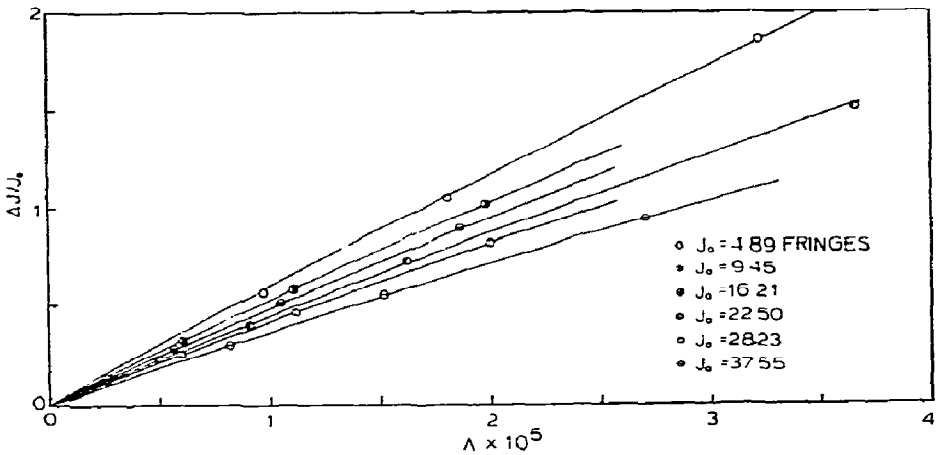

Fig. 3a

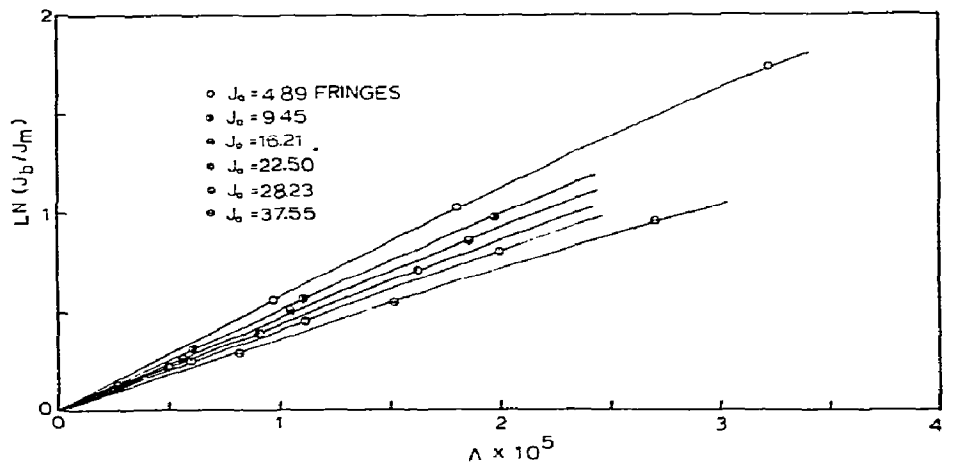

Fig. 3b

Fig. 3. Sedimentation equilibrium experiments at various speeds. Dextran T-70 Lot 7981. (a) Plots of $\Delta J/J_0$ vs Λ at constant J_0; these plots are required for the Albright and Williams [18] method. (b) Plots of ln (J_b/J_m) vs Λ at constant J_0. The limiting slope of each plot gives $M^0_{\text{w app}}$. Experiments performed with nonsector-shaped centerpieces are indicated by the half-filled circles.

or by

$$\frac{1}{M^0_{w\,app}} = \frac{1}{M_w} + B_{LS}c_0 + \ldots . \tag{25}$$

Thus, a plot of $1/M^0_{w\,app}$ vs c_0 has an intercept of $1/M_w$ and a limiting slope of B_{LS}. Fig. 3a shows plots of $\Delta J/J_0$ vs Λ for various values of c_0, and fig. 3b shows plots of $\ln J_b/J_m$ vs Λ. The limiting slope of either plot is $M^0_{w\,app}$ [see eq. (23)]. Fig. 4 shows the plots based on eq. (25); for each plot the slope is B_{LS} and the intercept is $1/M_w$. The values of B_{LS} and M_w obtained in this way are listed in table 2. Figs. 1 and 2 of the preliminary communication [1] show plots corresponding to figs. 3a and 4, respectively, for lot 7981.

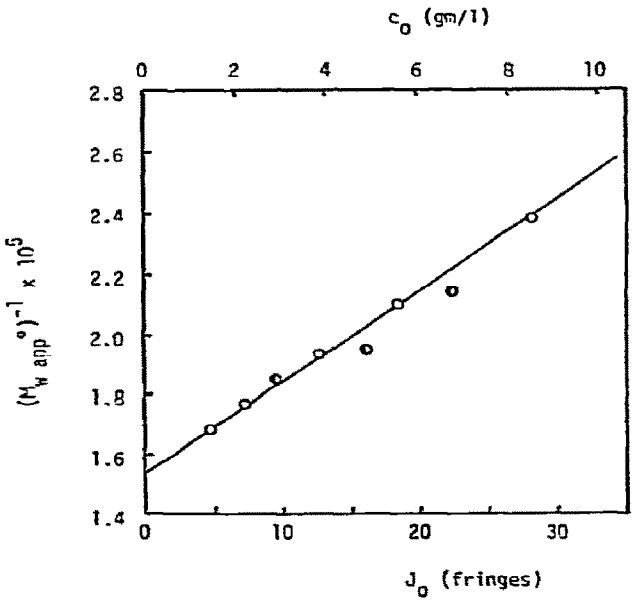

Fig. 4a

Fujita [15,16] has developed two methods for estimating B_{LS} from a series of sedimentation equilibrium experiments at one speed, provided Λ is constant. His first method stated that [15]

$$\frac{1}{M_{w\,cell\,app}} = \frac{1}{M_w} + B'c_0, \tag{26}$$

where

$$B' = B_{LS}\left(1 + \frac{\Lambda^2}{12}\frac{\Sigma_i\Sigma_k B'_{ik} f_i f_k M_i^2 M_k^2}{\Sigma_i\Sigma_k B'_{ik} f_i f_k M_i M_k}\right)$$

$$= B_{LS}(1 + \alpha'\Lambda^2) = B_{LS} + \alpha\Lambda^2. \tag{27}$$

Here the B'_{ik} are nonideal terms, and f_i and f_k are weight fractions of polymeric components i and k, whose molecular weights are M_i and M_k, respectively. The weight fraction of compoment $j (j = i$ or $k)$ are re-

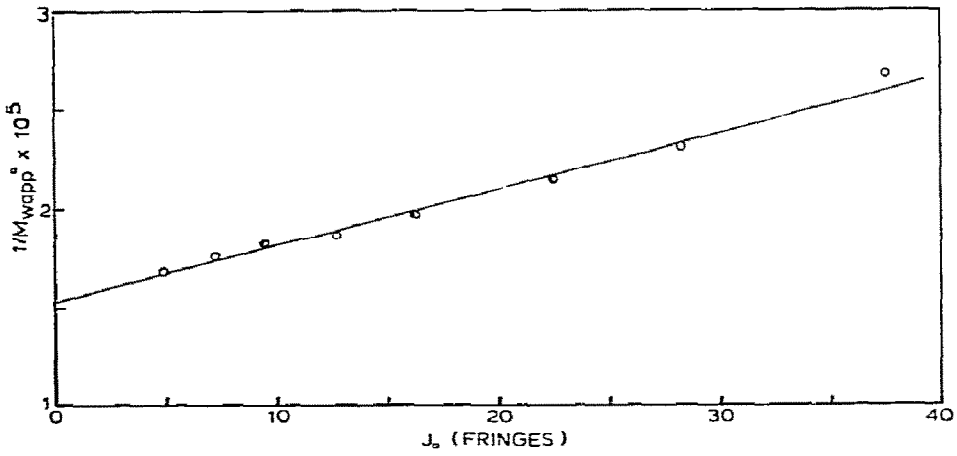

Fig. 4b

Fig. 4. Evaluation of M_w and B_{LS}. Plots of $1/M^0_{w\,app}$ vs J_0 are shown here. (a) This plot is based on fig. 3a. (b) This plot is based on fig. 3b. The intercept of these plots gives $1/M_w$ and the slope gives B_{LS}. Values of M_w and B_{LS} for fig. 4a are listed in table 2. With fig. 4b we obtained $M_w = 6.55 \times 10^4$ dalton and $B_{LS} = 0.291 \times 10^{-6}$ mole/(g) (fringe).

lated to the original concentrations of j, c_i^0, and to the total solute concentration, c_0, by the relation $f_j = c_j^0/c_0$. If all the B'_{ik} are the same for each polymeric component, then [15]

$$B' \approx B_{LS}(1 + \Lambda^2 M_z{}^2/12), \tag{28}$$

where [7,16,18,19]

$$B_{LS} = \frac{\Sigma_i \Sigma_k B'_{ik} f_i f_k M_i M_k}{\Sigma_i \Sigma_k f_i f_k M_i M_k}. \tag{29}$$

We have modified Fujita's second method [16] so that it states (see appendix A.2 for the derivation) that

$$\frac{1}{M_{w\ \text{cell app}}} = \frac{1}{M_w} + B^* \bar{c}, \tag{30}$$

where

$$\bar{c} = (c_b + c_m)/2, \tag{31}$$

$$B^* = B_{LS}(1 + \Delta) = B_{LS}(1 + \beta'\Lambda^2) = B_{LS} + \beta\Lambda^2, \tag{32}$$

and

$$\Delta = (\Lambda^2 M_w{}^2/12)\,[(M_z/M_w)^2 - (M_z/M_w)] = \beta'\Lambda^2. \tag{33}$$

It should be emphasized that $M_{w\ \text{cell app}}$, defined by eq. (18), has to be used with both of the Fujita methods [15,16]. These methods have been criticized since they require a prior knowledge or an estimate of M_z, if one expects to estimate M_w and B_{LS} from a series of experiments at constant Λ. It should be noted that Deonier and Williams [56] have shown for sector-shaped centerpieces that $\bar{c}$ is approximated by

$$\bar{c} \approx c_0\,[1 + (\Lambda^2 M_z{}^2/12)].$$

So, if the Fujita assumption [15,16] that all the B'_{ik} are equal, then the $B'c_0$ term in eq. (26) can be replaced by $B_{LS}\bar{c}$, which would make eq. (26) essentially the same as eq. (30). It is evident from eqs. (26) and (27) that at constant Λ, the limiting slope of a plot of $1/M_{w\ \text{app}}$ vs c_0 is B'. So, if values of B' are available from experiments performed at different speeds (several values of Λ^2), a plot of B' vs Λ^2 would have a slope of α and an intercept of B_{LS}. Both B_{LS} and $\alpha\Lambda^2$ can be used for the correction of the sedimentation equilibrium equation (see section 4) so that the MWDs can be obtained from nonideal solutions. Fig. 5a shows a plot of $1/(\Delta J/J_0)$ vs J_0 for various values of Λ; the slope of this plot is B'/Λ. Fig. 5b shows a plot of $1/(\Delta J/J_0)$ vs $\bar{J}$ for various values of Λ; the slope of this plot [see eq. (29)] is B^*/Λ. Fig. 6a and 6b show plots of B' vs Λ^2 and B^* vs Λ^2, respectively. The values of B', B^*, α, β and B_{LS} obtained by these methods are listed in table 2.

It is evident from both of the Fujita methods [15, 16], that at low speeds the values of B' or B^* can be calculated from two series of experiments. The values of B' or B^* obtained at two different values of Λ^2 can be set up as simultaneous equations, which can be used to estimate B_{LS} and also α and β. We have tested this idea using data obtained from experiments performed at three speeds; the results are tabulated in table 4. It appears from these data that good estimates of B_{LS} can be obtained in this way, but it is also apparent from this table that as the speed increases, the values of M_w become smaller, presumably due to complications arising from the redistribution of the polymeric components.

Values of M_z have also been calculated for these materials. There are two relatively simple ways to obtain $M_{z\ \text{app}}^0$, the apparent values of M_z. The first way is to use the more familiar equation, namely [4a,5,6a, 7,45,55]

$$M_{z\,\text{cell app}} = \frac{\left(\frac{1}{r}\frac{dc}{dr}\right)_{r_b} - \left(\frac{1}{r}\frac{dc}{dr}\right)_{r_m}}{2A(c_b - c_m)}, \tag{34}$$

where $A = (1 - \bar{v}\rho)\omega^2/2RT$. The other quantity which can be calculated is $M_{z\ \text{cell vol app}}$, which is defined by [4a,7,13,55]

$$M_{z\ \text{cell vol app}} = \frac{1}{\Lambda} \ln\left\{\left(\frac{1}{r}\frac{dc}{dr}\right)_{r_b} \left(\frac{1}{r}\frac{dc}{dr}\right)_{r_m}\right\}. \tag{35}$$

For an ideal, dilute solution $M_{z\ \text{cell app}}$ is the M_z of the polymeric solute. At real speeds with ideal, dilute solutions it has been shown that $M_{z\ \text{cell}} > M_{z\ \text{cell vol}}$ [55]. Similar arguments can be used to show that $M_{z\ \text{cell app}} > M_{z\ \text{cell vol app}}$. It can be shown, using procedures similar to those used by Fujita [15] in his derivation for B_{SD}, that

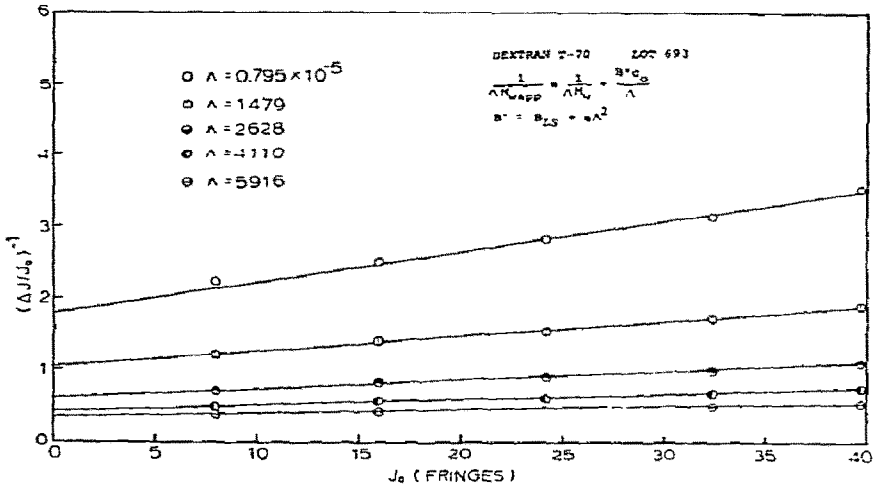

Fig. 5a

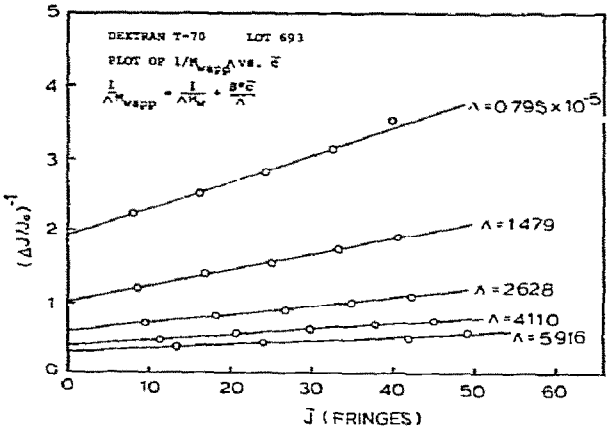

Fig. 5b

Fig. 5. Evaluation of B' and B^*. (a) Plot based on the first Fujita [15] method; the slope of this plot is B'/Λ. (b) Plot based on the second Fujita [16] method; the slope is B^*/Λ. Dextran T-70 Lot 693.

$$M_{z\,\text{cell app}}^{-1} = \frac{1}{M_z} + B_{SZ}(1+\gamma\Lambda^2)c_0 + \dots, \tag{36}$$

where

$$B_{SZ} = \frac{\Sigma_i\Sigma_k f_i f_k M_i M_k (M_i + M_k) B'_{ik}}{M_w M_z^2}, \tag{37}$$

and

$$\gamma = \frac{1}{12}\,\frac{\Sigma_i\Sigma_k f_i f_k M_i^2 M_k^2 (M_i + M_k) B'_{ik}}{\Sigma_i\Sigma_k f_i f_k M_i M_k (M_i + M_k) B'_{ik}}. \tag{38}$$

The derivation of eq. (36) is given in appendix A.3.

As $\Lambda \to 0$, one notes that

$$\lim_{\Lambda\to 0} M_{z\,\text{cell app}} = \lim_{\Lambda\to 0} M_{z\,\text{cell vol app}} = M_{z\,\text{app}}^0. \tag{39}$$

Table 4
Estimation of M_w, B_{LS} and α from experiments at three speeds using Fujita's [15] first method

A. Values of M_w

Rotor speed	$M_w \times 10^{-4}$ (dalton)	
(RPM)	Lot 7981	Lot 693
4400	6.59	6.71
6000	6.55	6.51
8000	6.25	6.43

B. Values of B_{LS} and α

Lot number	Speed combination (RPM)	$B_{LS} \times 10^6$ (mole ℓ/g²)	$\alpha \times 10^{-2}$ (ℓ/mole)
7981	4400 & 6000	1.06	0.804
	6000 & 8000	1.08	0.548
693	4400 & 6000	0.922	0.965
	6000 & 8000	0.899	2.05

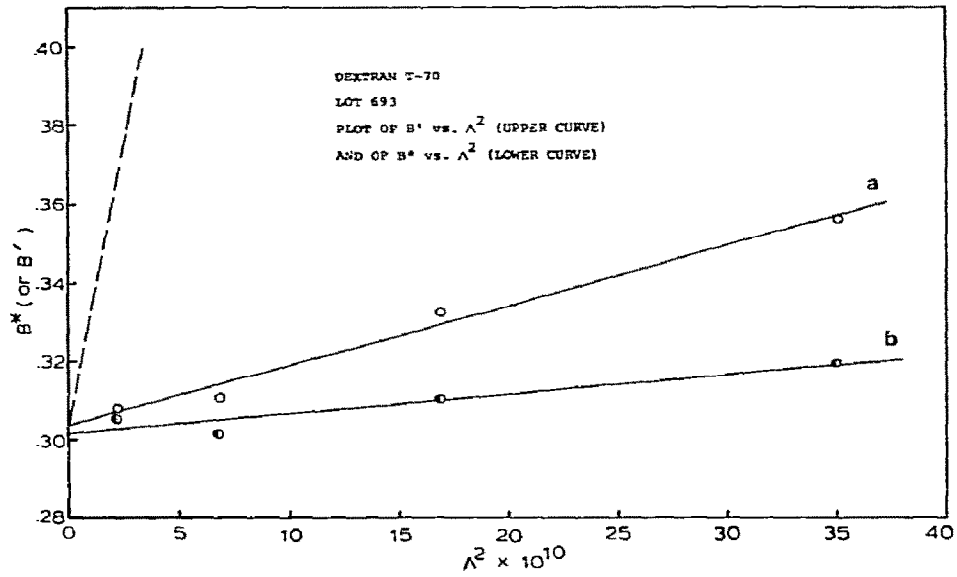

Fig. 6. Evaluation of α and β. (a) Values of B' obtained from the plots in fig. 5a were used here. The slope of a plot of B' vs Λ^2 is α. The dashed line intersecting this plot indicates the plot one would expect if all the B'_{ik} were equal. (b) Values of B^* obtained from fig. 5b were plotted against Λ^2, so that β could be obtained from the slope of this plot.

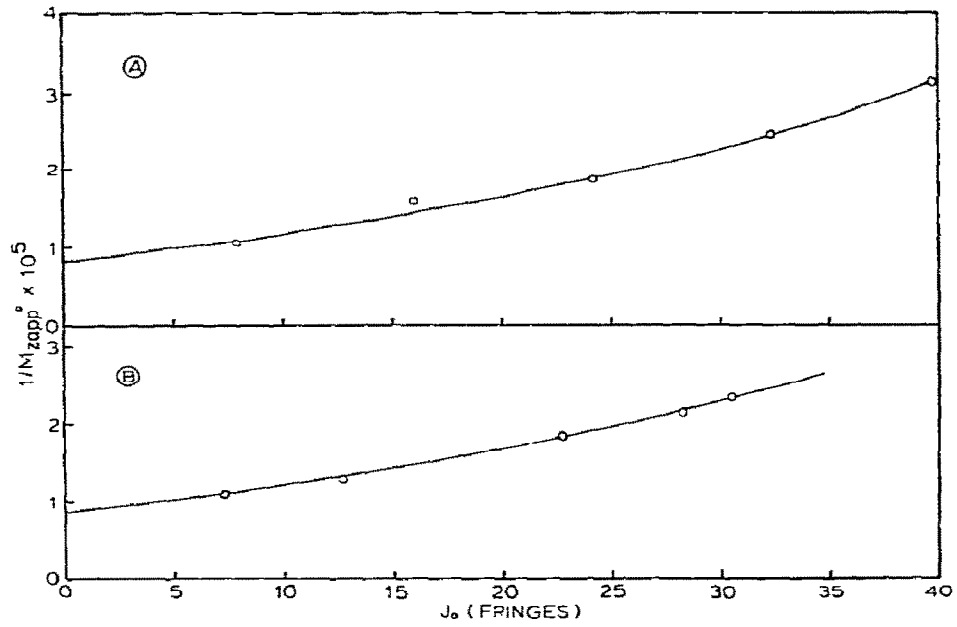

Fig. 7. Evaluation of M_z and B_{SZ}. The limiting slope of plots of $1/M^0_{z\,app}$ vs J_0 is B_{SZ}, and the intercept of each plot is $1/M_z$. Second order regression analysis was used to obtain the values of $1/M_z$ and B_{SZ}. (A) Lot 693. (B) Lot 7981.

A plot of $1/M^0_{z\ \mathrm{app}}$ vs c_0 [see eq. (36)] will have a slope of B_{SZ} and an intercept of $1/M_z$. Fig. 7 shows a plot of $1/M^0_{z\ \mathrm{app}}$ vs c_0 based on our measurements; the values of M_z and B_{SZ} that we obtained using eq. (34) are listed in table 2. It is also evident from eq. (36) that a plot of $1/M_{z\ \mathrm{cell\ app}}$ vs Λ^2 at constant c_0 will have a slope of $B_{SZ}\ \gamma$ and an intercept of $1/M^0_{z\ \mathrm{cell\ app}} = (1/M_z) + B_{SZ}c_0$.

3.4.2. Nonsector-shaped centerpieces

It is also possible to obtain $M_{w\ \mathrm{cell}}$, $M_{z\ \mathrm{cell}}$, or their apparent values from experiments performed using ultracentrifuge cells with nonsector-shaped centerpieces. In ideal, dilute solutions $M_{w\ \mathrm{cell}}$ is defined by [4a,7,13]

$$M_{w\ \mathrm{cell}} = \frac{\int_{r_m}^{r_b} M_{wr} c\, f(r)\, dr}{\int_{r_m}^{r_b} c\, f(r)\, dr} = \frac{\frac{1}{2A}\int_{c_m}^{c_b} \frac{f(r)\, dc}{r}}{c_0 \int_{r_m}^{r_b} f(r)\, dr}$$

$$= -\frac{1}{\Lambda c_0}\int_0^1 \frac{dc}{d\xi}\, dx. \qquad (40)$$

Here,

$$x = \int_{r_m}^{r} f(r)\, dr \Big/ \int_{r_m}^{r_b} f(r)\, dr, \qquad 0 \leqslant x \leqslant 1. \qquad (41)$$

The quantity $f(r)$ is the cross-sectional width of the cell holes, and x is the analog of ξ. If $f(r)$ is constant, then $x = (r - r_m)/(r_b - r_m)$. The equation for $M_{z\ \mathrm{cell}}$ is [4,55]

$$M_{z\ \mathrm{cell}} = \frac{\int_{c_m}^{c_b} \frac{M_{zr} f(r)\, dc}{r}}{\int_{c_m}^{c_b} f(r) \frac{dc}{r}} = \frac{\int_{c_m}^{c_b} \frac{f(r)\, d(cM_{wr})}{r}}{\int_{c_m}^{c_b} f(r) \frac{dc}{r}}$$

$$= \int_{c_m}^{c_b} f(r)\, d\left(\frac{1}{r}\frac{dc}{dr}\right) \Big/ \int_{c_m}^{c_b} f(r) \frac{dc}{r}. \qquad (42)$$

For nonideal solutions $M_{wr} = (1/A)\ [\mathrm{d} \ln c/\mathrm{d}(r^2)]$ becomes $M_{wr\ \mathrm{app}}$ and M_{zr} becomes $M_{zr\ \mathrm{app}}$, so that eqs. (40) and (42) define $M_{w\ \mathrm{cell\ app}}$ or $M_{z\ \mathrm{cell\ app}}$, respectively. The quantity $M_{w\ \mathrm{cell\ app}}$ can be expressed as

$$M_{w\ \mathrm{cell\ app}} = M_w \left\{1 - \left(\frac{1}{c_0 M_w} \times \int_0^1 \sum_i \sum_k c_{ir} c_{kr} M_i M_k B'_{ik}\, dx + \ldots\right)\right\}. \qquad (43)$$

Eq. (43) is easily obtained when one starts with eq. (A.5) in the appendix, which is identical with the Albright and Williams [18] eq. (3). Rearrangement of eq. (43) leads to

$$\frac{1}{M_{w\ \mathrm{cell\ app}}} = \frac{1}{M_w} + \frac{1}{c_0 M_w^2} \times \int_0^1 \sum_i \sum_k c_{ir} c_{kr} M_i M_k B'_{ik}\, dx + \ldots. \qquad (44)$$

As $\Lambda \to 0$, $c_{jr} \to c_j^0 (j = i \text{ or } k)$ and

$$\lim_{\Lambda \to 0} \frac{1}{M_{w\ \mathrm{app}}} = \frac{1}{M_w} + B_{LS} c_0, \qquad (45)$$

where

$$B_{LS} = \frac{\Sigma_i \Sigma_k f_i f_k M_i M_k B'_{ik}}{\Sigma_i \Sigma_k f_i f_k M_i M_k},$$

and

$$c_j^0 = f_j c_0 \qquad (j = i \text{ or } k).$$

For nonsector-shaped centerpieces the analog of $M_{w\ \mathrm{cell\ vol}}$ is [7,13]

$$M_{w\ \mathrm{cell\ vol}} = \int_{r_m}^{r_b} M_{wr} f(r)\, dr \Big/ \int_{r_m}^{r_b} f(r)\, dr. \qquad (46)$$

It is also possible to define $M_{z\ \mathrm{cell\ vol}}$ for cells with nonsector-shaped centerpieces, but this matter will not be pursued further in this paper.

To apply the Albright and Williams [18] method to cells with nonsector-shaped centerpieces, one plots $(-1/c_0)\int_0^1 (dc/d\xi)\, dx$ vs Λ [see eq. (40)] at constant c_0 to obtain $M^0_{w\ \mathrm{app}}$ from the limiting slopes of these

plots. Similarly, one could plot the ratio of the two integrals in eq. (42) vs $2A$ at constant c_0 and obtain $M^0_{z\,app}$ from the limiting slopes of these plots. Values of $1/M^0_{w\,app}$ are then plotted against c_0 to obtain $1/M_w$ as the intercept and B_{LS} as the slope. A similar reciprocal plot using $1/M^0_{z\,app}$ has $1/M_z$ as the intercept. It is not clear at present how to develop methods similar to the two Fujita methods [15,16] for evaluating B' or B^* [see eqs. (26) and (30)] for cells with nonsector-shaped centerpieces from experiments at two or three speeds.

Since there are various ways of averaging $M_{wr\,app}$ (or M_{wr} in ideal, dilute solutions) over the cell to obtain $M^0_{w\,app}$ (or M_w), one can apply eqs. (18) or (22) to cells with nonsector-shaped centerpieces. For these centerpieces eqs. (18) and (22) do not give $M_{w\,cell}$, $M_{w\,cell\,vol}$, or their apparent values at real speeds; however, in the limit of zero speed the equations will converge to $M^0_{w\,app}$ (or to M_w in ideal, dilute solutions). The advantage of using these equations in their simplicity; they are much easier to use than are eqs. (40) or (46), as they are evaluated by numerical integration. It is much easier to calculate $\Delta c/c_0$ than it is to calculate $(-1/c_0)\int_0^1 (dc/d\xi)dx$. We have tried the Albright and Williams [18] method with cells having nonsector-shaped centerpieces using $M^0_{w\,app}$ obtained by four methods [eqs. (18), (22), (40) and (46)]. Some results are shown in fig. 4.

4. Molecular weight distributions from ultracentrifugation

4.1. Correction of sedimentation equilibrium data for nonideal behavior

The theory for obtaining MWDs from sedimentation equilibrium experiments is described in detail elsewhere [4b,5,6b,7–13,24–26].

Here we indicate briefly how we corrected sedimentation equilibrium data, since this is the heart of our methods. We have used the same assumptions that Osterhoudt and Williams [18] and that Albright and Williams [19] have used for nonassociating, polymeric solutes in nonideal solutions to obtain the basic sedimentation equilibrium equation – see appendix A.1. Our starting equation is eq. (A.8) in the appendix, which can be rearranged to give

$$\frac{1}{M_{wr\,app}} = \frac{1}{M_{wr}} + \langle B'_{ik}\rangle_r c \tag{47}$$

The quantity $\langle B'_{ik}\rangle_r$ is defined by eq. (A.7). The problem in sedimentation equilibrium experiments is how to evaluate the nonideal term, $\langle B'_{ik}\rangle_r$. If we can make an estimate of $\langle B'_{ik}\rangle_r$, then we can estimate $[\mathrm{d}\ln c/\mathrm{d}(r^2)_{id}]$ or $[dc/d(r^2)]_{id}$. First note that

$$\frac{1}{M_{wr}} = \frac{1}{M_{wr\,app}} - \langle B'_{ik}\rangle_r c$$

$$= \frac{-1}{\left(\frac{1}{\Lambda}\frac{\mathrm{d}\ln c}{\mathrm{d}\xi}\right)_{id}} = \frac{1}{\left(\frac{1}{\Lambda}\frac{\mathrm{d}\ln c}{\mathrm{d}u}\right)_{id}}. \tag{48}$$

Here $M_{wr\,app}$ is defined by

$$\frac{1}{\Lambda}\frac{\mathrm{d}\ln c}{\mathrm{d}u} = \frac{-1}{\Lambda}\frac{\mathrm{d}\ln c}{\mathrm{d}\xi} = M_{wr\,app}.$$

To obtain $[dc/d(r^2)]_{id}$ one notes that

$$\frac{1}{c_{id}M_{wr}} = \frac{1}{c_{id}M_{wr\,app}} - \langle B'_{ik}\rangle_r \frac{c_r}{c_{id}}$$

$$= \frac{1}{\left(\frac{1}{\Lambda}\frac{dc}{du}\right)_{id}} = \frac{1}{\frac{c_{id}}{c_r}\left(\frac{1}{\Lambda}\frac{dc}{du}\right)} - \langle B'_{ik}\rangle_r \frac{c_r}{c_{id}}. \tag{49}$$

The subscript id refers to the values of $dc/d(r^2)$, c_r or $\mathrm{d}\ln c/\mathrm{d}(r^2)$ after correction for nonideal behavior.

There are basically four ways to estimate $\langle B'_{ik}\rangle_r$. Since we have shown in eq. (A.9) of the appendix that $\lim_{\Lambda\to 0}\langle B'_{ik}\rangle_r = B_{LS}$, so as a first approximation we assume that

$$\langle B'_{ik}\rangle_r \approx B_{LS}. \tag{50}$$

If all the B'_{ik} for the polymeric solutes were the same, this first assumption would be correct. The light scattering second virial coefficient can be obtained from the Albright and Williams [18] method or from the modifications to the Fujita methods which we suggested in the previous section [see eqs. (27) and (32)]. This first assumption neglects the effect of solute redistribution, due to the centrifugal field, on the nonideal term, $\langle B'_{ik}\rangle_r$. A second approximation makes an attempt to overcome this deficiency by assuming that

$$\langle B'_{ik}\rangle_r \approx B' = B_{LS}(1+\alpha'\Lambda^2) = B_{LS} + \alpha\Lambda^2, \qquad (51)$$

which is the same as eq. (27). In the discussion following eq. (32) we have shown how B' and α (or α') could be evaluated; fig. 5 and 6 show the plots required for the evaluation of these quantities. In table 4 we have also shown values of B_{LS} and α obtained from sedimentation equilibrium experiments at two different speeds.

The third approximation is to assume that

$$\langle B'_{ik}\rangle_r \approx B^* = B_{LS}(1+\beta'\Lambda^2) = B_{LS} + \beta\Lambda^2. \qquad (52)$$

We have shown in the preceeding section [see the discussion following eq. (32), as well as figs. 5 and 6] how β (or β') can be evaluated.

The fourth approximation to the evaluation of $\langle B'_{ik}\rangle_r$ is to assume that the $\langle B'_{ik}\rangle_r$ could be replaced by its value at a radial position where $u = 1/2$ or where $c = \bar{c}$ ($\bar{c} = [c_b + c_m]/2$). The value of $\langle B'_{ik}\rangle_{\bar{c}}$ can be estimated using the eq. (A.31), if $\Lambda M_z < 2\pi$ and $\Lambda M_{z+1} < 2\pi$; for the case where $u = 1/2$, $r = \sqrt{\frac{1}{2}(r_b^2 + r_m^2)}$, and $\langle B'_{ik}\rangle_{u=1/2}$ is approximated by (see appendix A.5)

$$\langle B'_{ik}\rangle_{u=1/2} = \frac{B_{LS}(1-\alpha'[M_{z+1}/M_z]\Lambda^2 + \ldots),}{1 - \Lambda^2 M_z M_{z+1}/12 + \ldots}, \qquad (53)$$

when $\Lambda M_z < 2\pi$ and $\Lambda M_{z+1} < 2\pi$. We have shown in the preceeding section how α' and M_z can be evaluated; M_{z+1} would have to be estimated from the MWD calculated by one of the preceeding methods.

In order to use Donnelly's [24,25] method or one form of Scholte's [26–28] method, it is necessary to have an estimate of c_{id} ($c_{id} = c_{r\ ideal}$). This estimate is obtained from the conservation of mass equation when refractometric optics are used. First it is necessary to obtain values of $[c_r/c_m]_{id}$ or $[c_r/c_b]_{id}$ from the relations

$$\ln (c_r/c_m)_{id} = \int_{r_m}^{r} \left(\frac{d \ln c}{d(r^2)}\right)_{id} d(r^2), \qquad (54)$$

or

$$\ln(c_r/c_b)_{id} = \int_{r_b}^{r} \left(\frac{d \ln c}{d(r^2)}\right)_{id} d(r^2). \qquad (55)$$

These values of $(c_r/c_m)_{id}$ or $(c_r/c_b)_{id}$ are then inserted into the appropriate conservation of mass equations, which depend on the shape of the centerpiece, to obtain $(c_m)_{id}$ or $(c_b)_{id}$. For a sector-shaped centerpiece the following relations apply:

$$\frac{c_0}{(c_m)_{id}} = \frac{1}{(r_b^2 - r_m^2)} \int_{r_m}^{r_b} \left(\frac{c_r}{c_m}\right)_{id} d(r^2)$$

$$= \int_0^1 \left(\frac{c_r}{c_m}\right)_{id} du, \qquad (56)$$

$$\frac{c_0}{(c_b)_{id}} = \frac{1}{(r_b^2 - r_m^2)} \int_{r_m}^{r_b} \left(\frac{c_r}{c_b}\right)_{id} d(r^2) = \int_0^1 \left(\frac{c_r}{c_b}\right) du. \qquad (57)$$

For a nonsector-shaped centerpiece the conservation of mass equations are

$$\frac{c_0}{(c_m)_{id}} = \int_0^1 \left(\frac{c_r}{c_m}\right)_{id} dx \qquad (58)$$

and

$$\frac{c_0}{(c_b)_{id}} = \int_0^1 \left(\frac{c_r}{c_b}\right)_{id} dx, \qquad (59)$$

where x is defined by eq. (41). Once values of $(c_r)_{id}$, $(dc/dr)_{id}$ and $(d \ln c/d(r^2))_{id}$ are available, then we can use any method based on ideal, dilute solutions to evaluate the MWD.

At the higher speeds required by Scholte's [26–28] methods, we may not be able to obtain values of dc/dr or c_r near the bottom of the cell, so we will have to make an estimate of $(c_m)_{id}$ in order to obtain $(dc/d(r^2))_{id}$ [see eq. (49)]. This can be done by plotting $\ln (c_m)_{id}$ vs Λ (obtained at lower speeds) and estimating the value of c_m at the higher speeds from the trend of this plot. Alternatively, if the MWD be unimodal, then $f(M)$ can be estimated by Donnelly's [24,25] method, and c_m (or any other $(c_r)_{id}$) could be estimated from the appropriate equations for the concentration distributions at sedimentation equilibrium [see eqs. (63), (76), (78) or (92)].

4.2. MWDs by Donnelly's method

Donnelly [24,25] showed that the equation for the concentration distribution at sedimentation equilibrium could be converted into a Laplace transform. If an analytical expression for this transform can be found, then the MWD can be obtained from the inverse of the Laplace transform. Since the concentration and concentration gradient equations depend on the shape of the centerpieces, we will consider the results obtained from experiments using each centerpiece separately.

4.2.1. Sector-shaped centerpieces

For sector-shaped centerpieces Donnelly [24,25] showed that if the following substitutions are made;

$$t = \Lambda M, \tag{60}$$

$$\xi = (r_b^2 - r^2)/(r_b^2 - r_m^2) = s, \tag{61}$$

and

$$\phi(t) = \frac{\Lambda M f(M)}{1 - \exp(-\Lambda M)}, \tag{62}$$

then the concentration distribution, $\theta(\xi) = c_r/c_0$, could be converted to a Laplace transform. In the equations to follow $\theta(\xi)$ will be used with corrected and uncorrected data so that the differences between ideal and nonideal conditions can be illustrated. Thus

$$\Lambda\theta(\xi) = \Lambda(c_r/c_0) = \int_0^\infty \frac{\Lambda M f(M) \exp(-\Lambda M\xi)\, d(\Lambda M)}{1 - \exp(-\Lambda M)}$$

$$= \int_0^\infty \phi(t)\, e^{-st}\, dt = L\{\phi(t)\}. \tag{63}$$

Here $L\{\phi(t)\}$ is the Laplace transform of $\phi(t)$. In order to use the Laplace transform method we must use the experimental data to obtain an analytical expression for $L\{\phi(t)\}$. The first step is to make a plot of $F(n,\mu)$ vs u. Here

$$F(n,\mu) = 1/(d \ln c/d(r^2)) = b/(d \ln c/du), \tag{64}$$

$$b = (r_b^2 - r_m^2), \tag{65}$$

and

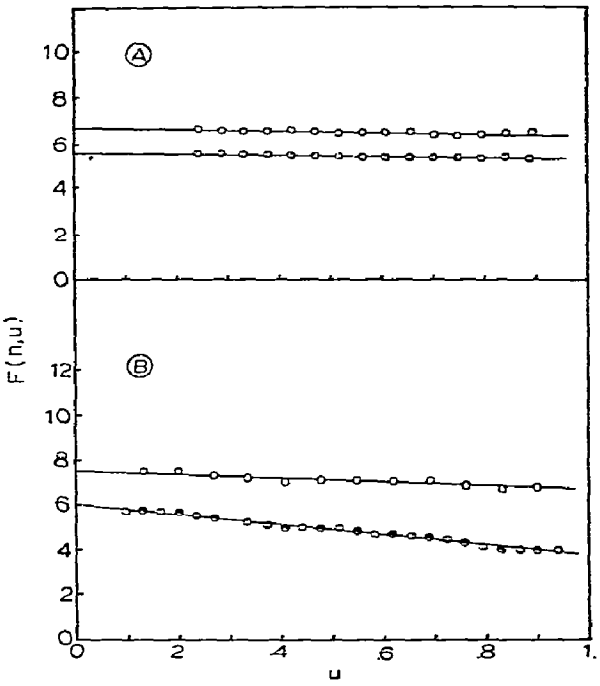

Fig. 8. Plots of $F(n,\mu)$ vs u. These plots, based on data collected at 6000 RPM, are required for the evaluation of MWDs by Donnelly's method [24,25]. (a) Nonsector-shaped centerpiece. Lot 7981. Upper plot: No correction for nonideality. Lower plot: This plot is based on data corrected for nonideality by Method I [see eq. (50)]. (b) Sector-shaped centerpiece. Lot 693. Upper plot: No correction for nonideality. Lower plot: Corrected for nonideal behavior by Method I (Φ) and by Method II (Θ). The line drawn through these points is the line of regression for the data corrected by Method I. Values of P and Q obtained by various methods for correcting for nonideal behavior are listed in table 5.

$$u = (r^2 - r_m^2)/(r_b^2 - r_m^2) = 1 - \xi = 1 - s. \tag{66}$$

Fig. 8 shows plots of $F(n,\mu)$ vs u for uncorrected and corrected data. The effect of various methods of correction is shown in this figure. It can be shown that [7,24,25]

$$\Lambda\theta(\xi) = \frac{1}{K}\left(\frac{c(u)}{c(u=0)}\right) = \frac{1}{K} \exp \int_0^u \frac{b\,du}{F(n,\mu)}$$

$$= f(u) = f(s) = L\{\phi(t)\}. \tag{67}$$

Here,

$$1/K = \Lambda[c(u=0)/c_0] \tag{68}$$

Table 5
Values of P and Q required by Donnelly's method for MWD

Speed	4400 RPM		6000 RPM		8000 RPM		10000 RPM	
	P	Q	P	Q	P	Q	P	Q
A. Lot 7981								
1. Nonsector-shaped centerpiece								
Nonideal	12.474	0.870	6.668	0.299	3.928	0.340		
Corrected for nonideality by method I [eq. (50)]	9.863	1.708	5.468	1.142	3.438	1.197		
2. Sector-shaped centerpiece								
Nonideal	13.480	0.187	7.403	0.161	4.071	0.421		
Corrected for nonideality by method I [eq. (50)]	8.909	1.166	5.265	1.192	3.170	0.925		
B. Lot 693								
Sector-shaped centerpiece only								
Nonideal	13.593	1.087	7.523	0.864	4.518	0.644	3.180	0.642
Corrected for nonideality by method I [eq. (50)]	10.229	2.552	6.071	2.335	4.020	2.068	3.085	1.963
Method II [eq. (51)]	10.218	2.557	6.055	2.351	4.002	2.117	3.077	2.076
Method III [eq. (52)]	10.225	2.554	6.065	2.340	4.014	2.084	3.082	2.001
Method IV [eq. (53)]	9.998	2.653	5.651	2.759				
Method V [eq. (A.31)]	10.607	2.387	6.507	1.893				

For the plots shown in fig. 8 we obtained the following equation for $F(n, u)$:

$$F(n,u) = P - Qu. \tag{69}$$

Here $-Q$ is the slope and P is the intercept of these plots; the values of P and Q obtained from these plots are listed in table 5. When $F(n,u) = P - Qu$, it has been shown that [7,24,25]

$$L\{\phi(t)\} = \frac{(P/Q)^{b/Q}}{K} \frac{1}{(s+a)^n}, \tag{70}$$

where

$$n = b/Q \tag{71}$$

and

$$a = (P/Q) - 1. \tag{72}$$

Donnelly [7,24,25] showed that the inverse of this Laplace transform was

$$\phi(t) = \frac{(P/Q)^{b/Q}}{K} \frac{t^{[(b/Q)-1]}}{\Gamma(b/Q)} e^{-t(P/Q-1)}. \tag{73}$$

Here $\Gamma(b/Q)$ is the gamma function of b/Q. Once $\phi(t)$ is known, $f(M)$ can be obtained for these experiments; $f(M)$ is given by

$$f(M) = \frac{(P/Q)^{b/Q}}{K} \frac{t^{[(b/Q)-2]}}{\Gamma(b/Q)} e^{-t(P/Q-1)} (1 - e^{-t}). \tag{74}$$

Fig. 9a and 9b show plots of $f(M)$ vs M that we obtained at different speeds from these experiments using uncorrected data. In these figures we have also displayed the results obtained by the manufacturer (dashed line), who provided information sheets showing the MWD they obtained using analytical gel chromatography and light scattering. Note how the MWDs obtained from uncorrected plots of $F(n,u)$ vs u (see fig. 8) differ from the manufacturer's (Pharmacia Fine Chemicals) MWDs. The correction for nonideality using the first method

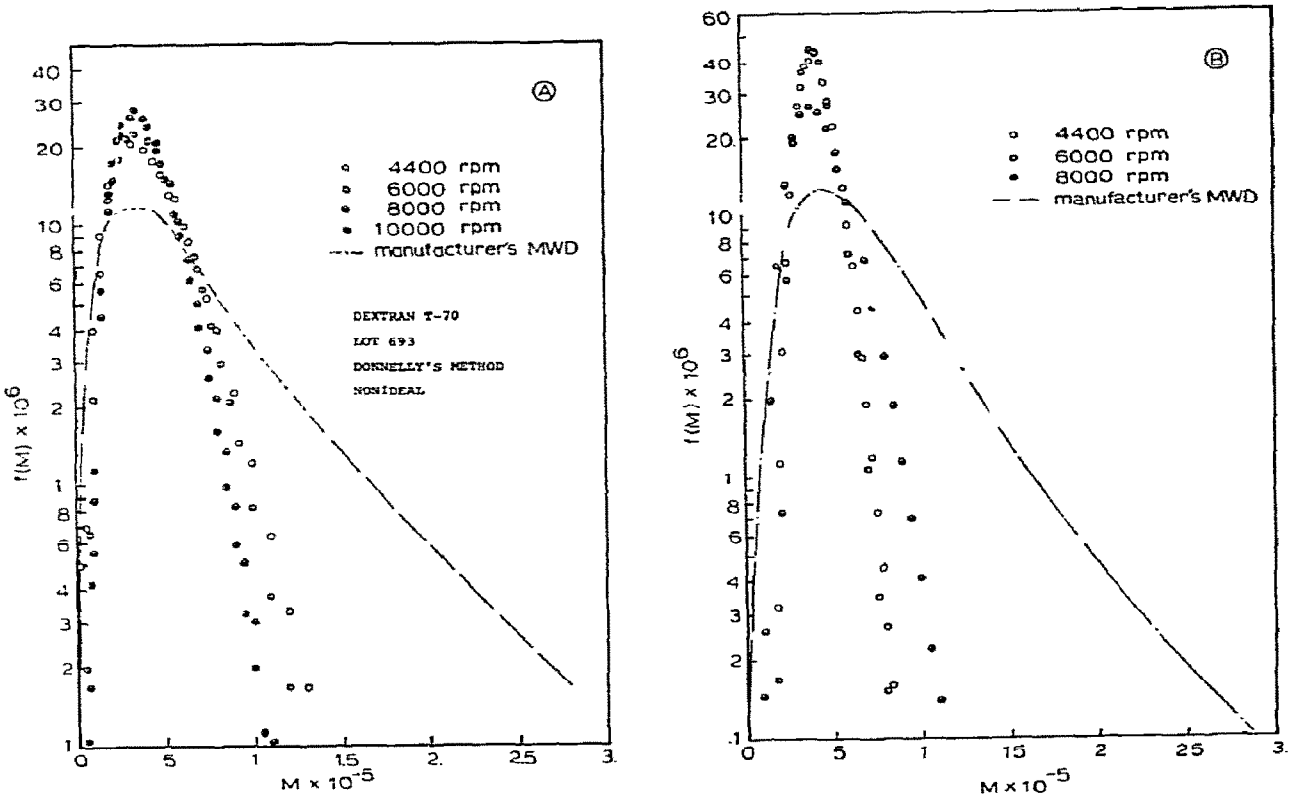

Fig. 9. Uncorrected differential MWDs at various speeds. Donnelly's method [24,25]. Sector-shaped centerpieces. The values of $f(M)$ vs M shown here for different speeds from uncorrected plots of $F(n,u)$ vs u (see fig. 8b). The manufacturer's MWD, obtained by analytical gel chromatography and light scattering, is indicated by the dashed curve. Note the difference between the manufacturer's MWD and the uncorrected MWDs. (a) Lot 693. (b) Lot 7981.

[see eqs. (48) and (50)] gives quite a dramatic change. This is evident in figs. 10a and 10b, where the corrected MWDs for experiments at various speeds are plotted along with the manufacturer's MWD (dashed line). Here our MWDs give good agreement with the manufacturer's MWD. Fig. 10a (lot 693) indicates very little, if any, speed effect after correction for B_{LS}; on the other hand fig. 10b shows that there is still a slight speed effect with lot 7981 after correction for B_{LS}. It is quite evident from figs. 8–10 that the plots of $f(M)$ vs M are quite sensitive to the plots of $F(n,u)$ vs u.

If all the B'_{ik} were equal, the first model for nonideal behavior would be correct, and there would be no difference in the corrected MWDs at different speeds. Furthermore, the values of M_n, M_w and M_z calculated from the MWD should give good agreement with the independently determined values of these quantities. The results of the application of the second and third methods for nonideal correction to the MWD for the dextran lot 693 are shown in figs. 11a and 11b, respectively; results at various speeds are displayed in these figures. We have not displayed any plots showing the MWDs obtained using the estimated values for $(B'_{ik})_r$ at $u = 1/2$ or at the radial position for which $c = \bar{c}$, since these methods for nonideal correction are restricted to lower speeds (8000 RPM or less for these dextrans).

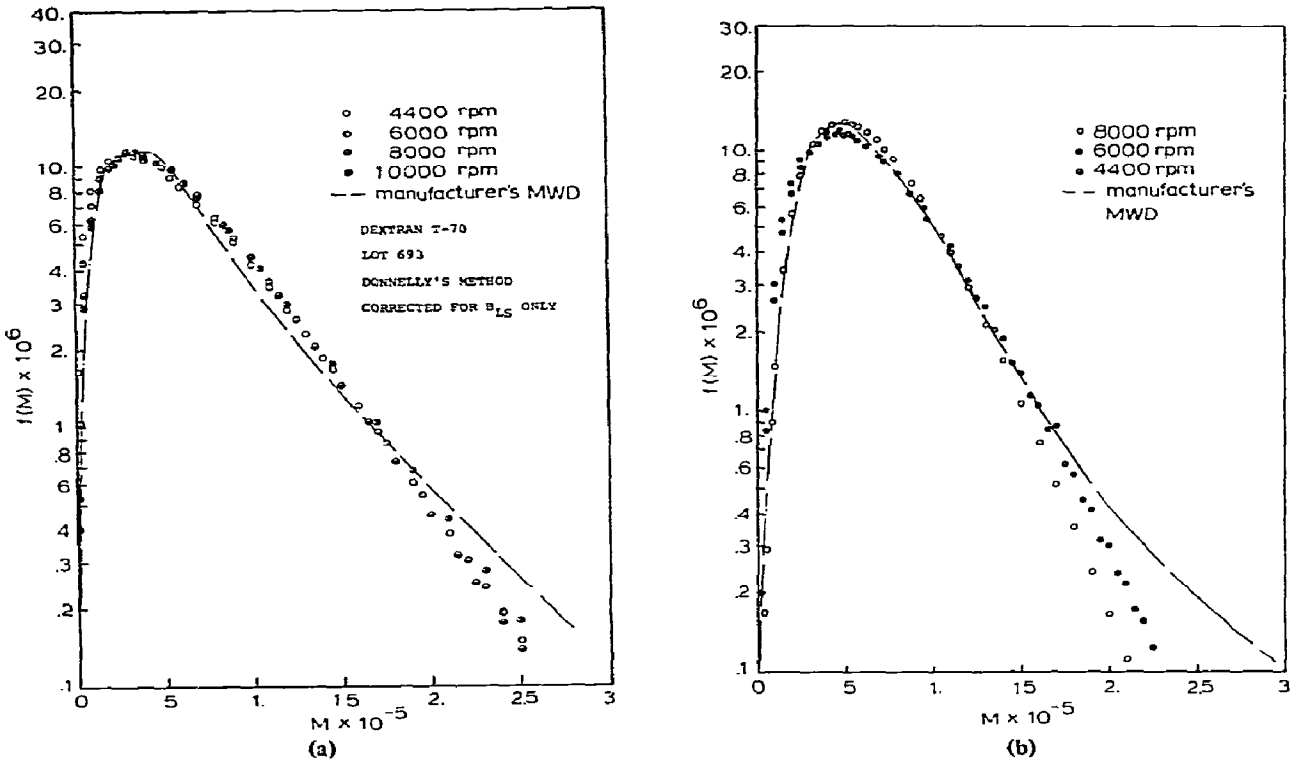

Fig. 10. MWDs by Donnelly's method [24,25] using data corrected for nonideality by Method I [see eq. (50)]. Sector-shaped centerpieces. Results at several speeds are shown here along with the manufacturer's MWD (dashed line). (a) Lot 693. (b) Lot 7981.

4.2.2. Nonsector-shaped centerpieces

If one makes the following substitutions

$$t = \Lambda M, \tag{60}$$

$$\xi = s, \tag{61}$$

and

$$\gamma(t) = f(M) / \int_0^1 \exp(-\Lambda M \xi)\, dx, \tag{75}$$

then the concentration distribution, $\hat{\theta}(\xi) = c_r/c_0$, at sedimentation equilibrium for a nonassociating, polymeric solute can be converted into a Laplace transform, $L\{\gamma(t)\}$. Thus,

$$\Lambda\hat{\theta}(\xi) = \Lambda[c_r/c_0] = \int_0^\infty \frac{f(M)\exp(-\Lambda M\xi)\, d(\Lambda M)}{\int_0^1 [\exp(-\Lambda M\xi)]\, dx}$$

$$= \int_0^\infty \gamma(t)\, e^{-st}\, dt = L\{\gamma(t)\}. \tag{76}$$

Here x is an analog of ξ, and it is defined by eq. (41). In order to obtain an analytical expression for $L\{\gamma(t)\}$ it is necessary to make a plot of $F(n,u)$ vs u. The circumflex, $\hat{}$, in eq. (76) indicates that we are dealing with a nonsector-shaped centerpiece. For nonsector-shaped cells we used the first approximation only, i.e., $\langle B'_{ik}\rangle_r \approx B_{LS}$, since it is unclear at present how to obtain the other quantities needed to include a speed effect with these centerpieces. In our experiments the corrected and uncorrected plots of $F(n,u)$ vs u had an equation of the form

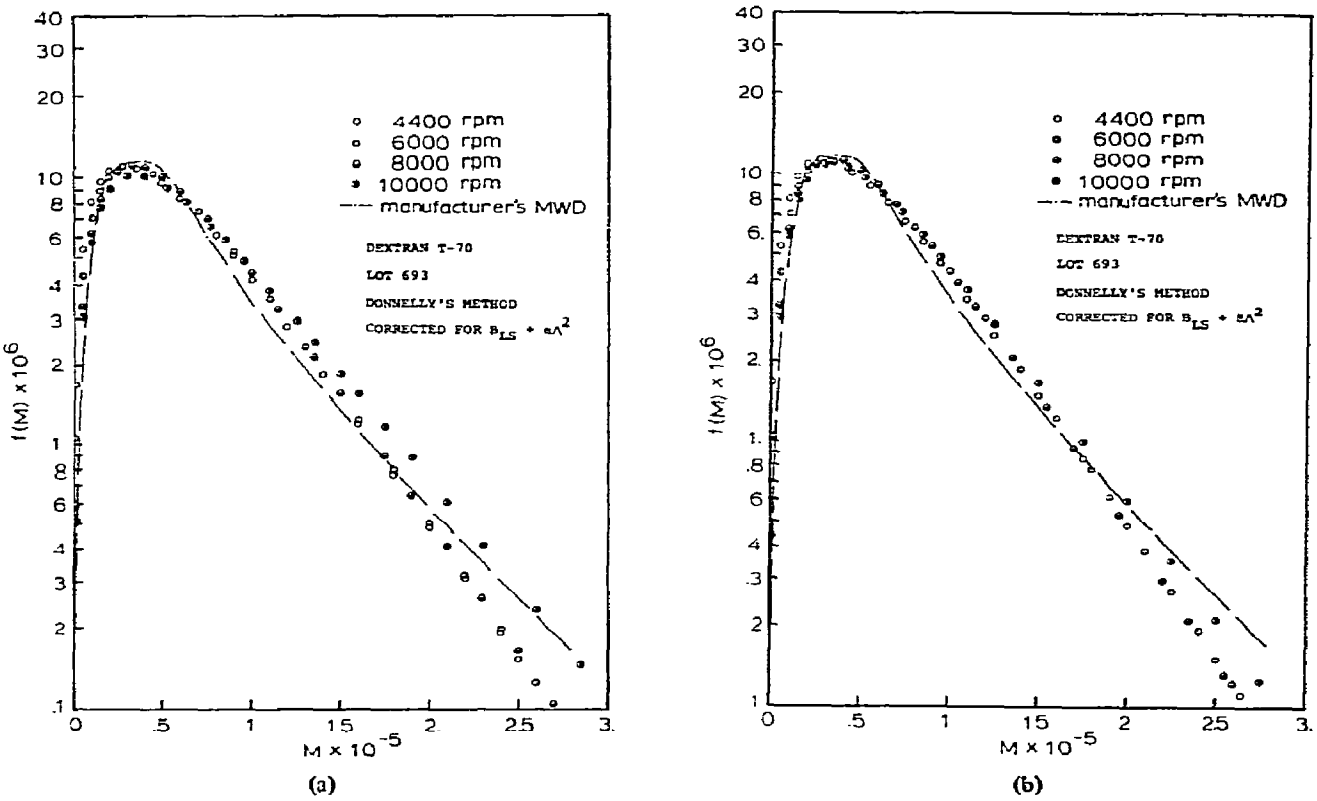

Fig. 11. MWDs by Donnelly's method [24,25] using data corrected for nonideality. Sector-shaped centerpieces. (a) Corrected by Method II [see eq. (51)]. (b) Corrected by Method III [see eq. (52)]. Results for lot 693 at several speeds are shown along with the manufacturer's MWD (dashed line).

$$F(n,u) = P - Qu, \tag{68}$$

which is the same type of equation obtained with sector-shaped centerpieces. The plots of $F(n,u)$ vs u for this centerpiece are displayed in fig. 8 also. The values of P and Q obtained in these experiments are also listed in table 5. The Laplace transform is the same as we obtained with sector-shaped centerpieces [see eq. (70)]. Hence the MWD is given by [7]

$$f(M) = \left(\int_0^1 [\exp(-\Lambda M\xi)]\, dx \right) \gamma(t)$$

$$= \left(\int_0^1 [\exp(-\Lambda M\xi)]\, dx \right) \frac{(P/Q)^{b/Q}}{K}$$

$$\times \frac{t^{(b/Q-1)}}{\Gamma(b/Q)}\, e^{-t(P/Q-1)}. \tag{77}$$

Corrected and uncorrected plots of $f(M)$ vs M are shown in fig. 12. The results are quite similar to those obtained with sector-shaped centerpieces. These experiments were carried out with the dextran T-70 lot 7981. Correction for nonideality, using B_{LS} [see eq. (50)], gives good agreement with the manufacturer's MWD, whereas the uncorrected plot does not resemble the other two plots.

4.3. MWD by Scholte's method

4.3.1. Sector-shaped centerpieces

For these centerpieces the concentration and the concentration gradient distributions can be expressed as [26–28]

$$\theta(\xi) = \frac{c(\xi)}{c_0} \sum_i \frac{\Lambda M_i f_i \exp(-\Lambda M_i \xi)}{1 - \exp(-\Lambda M_i)}, \tag{78}$$

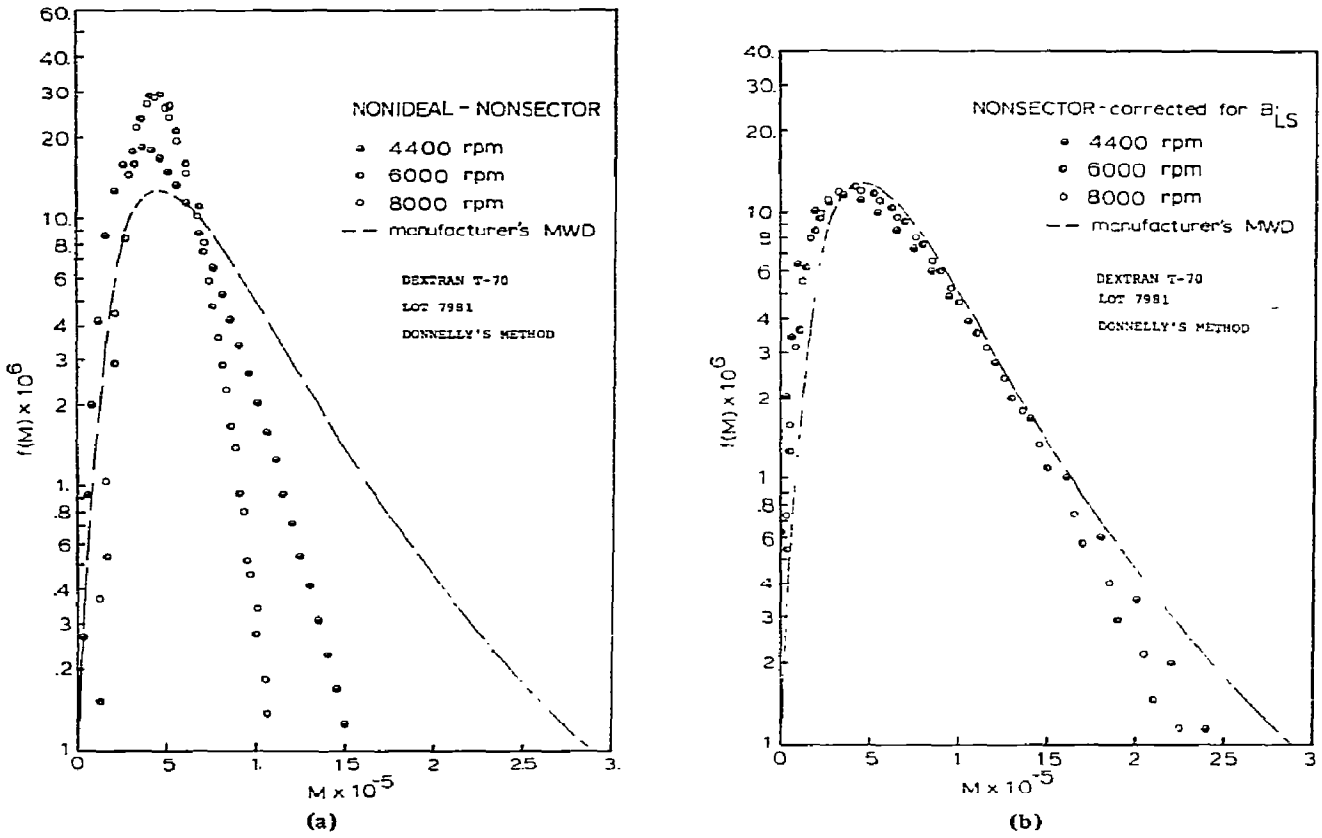

Fig. 12. MWDs by Donnelly's method [24,25]. Nonsector-shaped centerpieces. Lot 7981. (a) MWDs obtained at various speeds using uncorrected plots of $F(n,u)$ vs u (see fig. 8a). (b) MWDs obtained at various speeds using data corrected for nonideal behavior by Method I [see eq. (50)]. Note the pronounced difference between figs. 12a and 12b.

and

$$-\theta'(\xi) = \frac{-1}{c_0}\frac{dc}{d\xi} = \sum_i \frac{\Lambda^2 M_i^2 f_i \exp(-\Lambda M_i \xi)}{1-\exp(-\Lambda M_i)} = U(\Lambda,\xi). \tag{79}$$

Here a discrete distribution is used instead of a continuous distribution required by Donnelly's method [24, 25]. Scholte expressed $U(\Lambda,\xi)$ as an array of linear equations of the type

$$U(\Lambda,\xi)_j = \sum_i f_i K_{ij} + \delta_j, \tag{80}$$

where

$$K_{ij} = \frac{\Lambda_j^2 M_i^2 \exp(-\Lambda_j M_i \xi)}{1-\exp(-\Lambda_j M_i)}, \tag{81}$$

and

$$\xi = (r_b^2 - r^2)/(r_b^2 - r_m^2), \quad 0 \leqslant \xi \leqslant 1. \tag{82}$$

The quantity δ_j is a measure of the experimental error. Sedimentation equilibrium experiments on the same solution are performed at different speeds so that an array of $U(\Lambda,\xi)_j$ can be set up and solved for the f_i, the weight fraction of component i. The subscript j indicates that Λ [defined by eq. (19)] depends on speed; the subscript i indicates that the variable is independent of speed.

In order to solve for the f_i one first sets up a table of $U(\Lambda,\xi)_j$ at five radial positions (if possible) – at $\xi = 1$ (the air-solution meniscus), $\xi = 3/4$, $\xi = 1/2$, $\xi = 1/4$ and $\xi = 0$ (the radial position of the cell bottom) – for each value of Λ_j. Table 2 of ref. [27] shows how a

data table for Scholte's method is set up. At higher speeds (higher values of Λ) it may not be possible to obtain values of $U(\Lambda,\xi)$ at $\xi = 0$ and $\xi = 1/4$, so these spaces are left blank in the data table. The next step is to assume a series or grid of molecular weights, M_i, that covers the range of molecular weights in the polymer sample. Scholte [26–28] showed that for best results the interval between the successive M_i should be logarithmic; usually $M_j = 2M_i$, although the logarithmic interval can be between 1.8 and 2.5. In this work we used $M_j = 2M_i$. Once a first series of molecular weights is chosen, one solves for the f_i by linear programming. This method is nicely set up for linear programming, since (1) the sum of all weight fractions must be one ($\Sigma_i f_i = 1$), (2) only positive numbers are involved (for any f_i, $0 \leqslant f_i \leqslant 1$) so that we have a set of linear equations with no negative values, and (3) the choice of f_i not only satisfies condition 2, but it must also lead to $\Sigma_j|\delta_j|$ being a minimum.

The first series is not unique; other choices of M_i could also be used. With good experimental data four series of M_i can be used. The second series of M_i is chosen by multiplying each M_i in the first series by $2^{1/4}$. For the third series one multiplies the first series by M_i by $2^{1/2}$, and for the fourth series of M_i the multiplier is $2^{3/4}$. For each series of M_i an array of $U(\Lambda,\xi)_i$ is constructed, and one solves for the f_i by linear programming. One can construct a table of f_i and M_i for each series [26–28].

In order to obtain the MWD one notes that

$$\sum_i f_i \text{ (any one series)} = 1. \tag{83}$$

For the four series of M_i

$$\sum_i f_i \text{ (all four series)} = 4, \tag{84}$$

and

$$\sum_i (f_i/4) \text{ (all four series)} = 1. \tag{85}$$

With a continuous MWD f_i is replaced by $f(M)\,dM$, and

$$\sum_i f_i = \int_0^\infty f(M)\,dM = 1. \tag{86}$$

This integral can also be written as

$$\int_0^\infty f(M)\,dM = \int_0^\infty M f(M)\frac{dM}{M} = 1. \tag{87}$$

If the second integral in eq. (87) is evaluated numerically, one notes that

$$\int_0^\infty M f(M)\frac{dM}{M} \approx \Delta \ln M \sum_i [M f(M)]_i = 1. \tag{88}$$

When the data for all four series are combined, it follows that

$$\Delta \ln M = \ln M_j - \ln M_i = \ln (2^{1/4}) = 0.693/4. \tag{89}$$

One also notes that

$$\sum_i [M f(M)]_i = 4/0.693. \tag{90}$$

Because of eqs. (89) and (90), it follows that

$$[M f(M)]_i = f_i/0.693, \tag{91}$$

when data for all four series are used. This procedure has been followed, and the results are shown in fig. 13. Both corrected [using the first method for nonideal correction – see eq. (50)] and uncorrected results are shown for lot 693 in this figure. Some results we obtained with lot 7981 are shown in fig. 4 of the preliminary communication [1]. Because of the high speeds required by Scholte's method [26–28], we have restricted our nonideal corrections to the first model only. The results shown in fig. 13 are based on data obtained at three speeds. Although experiments have been performed at seven speeds, we have not been able to obtain good results when all speeds were included.

4.3.2. Nonsector-shaped centerpieces

With these centerpieces the concentration and concentration gradient distribution becomes [7]

$$\theta(\xi) = \sum_i \frac{f_i \exp(-\Lambda M_i \xi)}{\int_0^1 \exp(-\Lambda M_i \xi)\,d\xi} = \frac{c(\xi)}{c_0}, \tag{92}$$

and

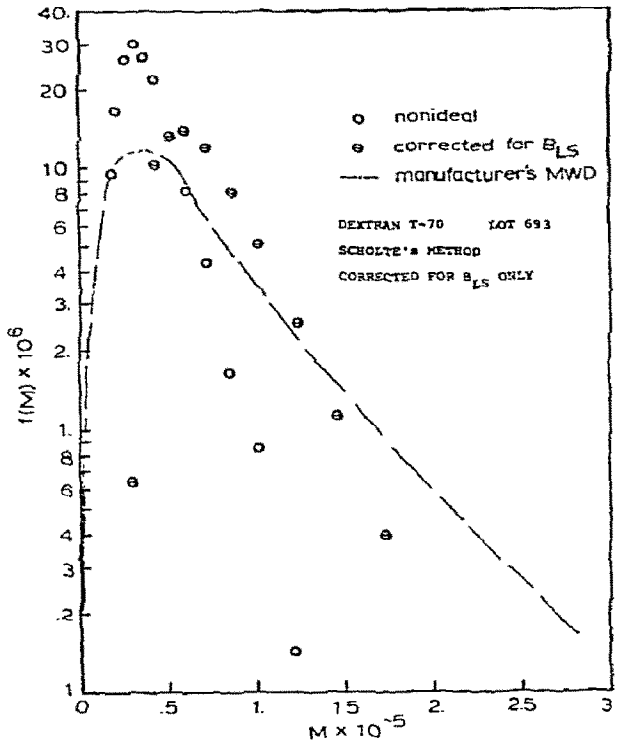

Fig. 13. MWDs by Scholte's method [26–28]. Sector-shaped centerpieces. Lot 693. Both corrected (by Method I) and uncorrected MWDs are shown here along with the manufacturer's MWD (dashed line).

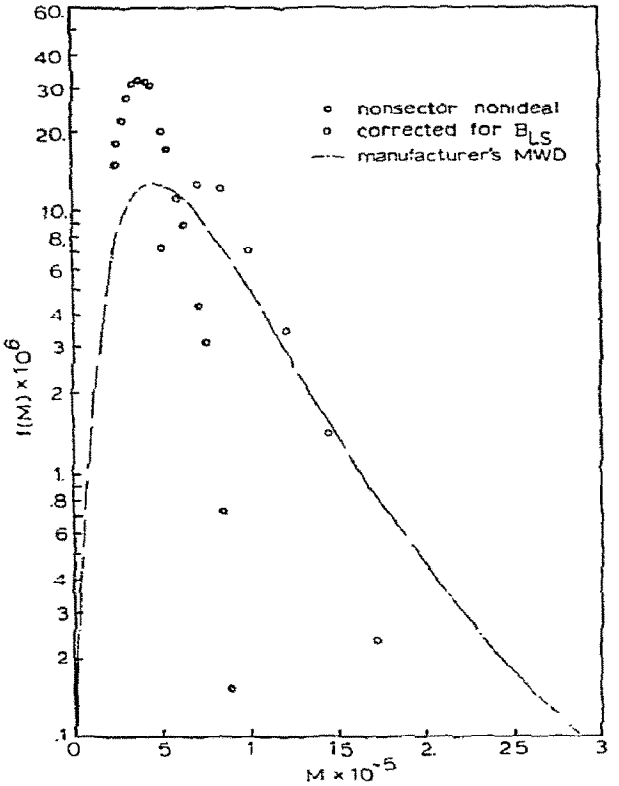

Fig. 14. MWDs by Scholte's method [26–28]. Nonsector-shaped centerpiece. Lot 7981. Both corrected (by Method I only) and uncorrected MWDs are shown along with the manufacturer's MWD (dashed line).

$$-\hat{\theta}'(\xi) = \frac{-1}{c_0}\frac{dc}{d\xi} = \sum_i \frac{\Lambda M_i f_i \exp(-\Lambda M_i \xi)}{\int_0^1 \exp(-\Lambda M_i \xi)\, dx}. \qquad (93)$$

Here x is the analog of ξ for a nonsector-shaped centerpiece; it is defined by eq. (41). The analog of eq. (79) is

$$V(\Lambda, \xi)_j = \sum_i f_i H_{ij} + \delta_j, \qquad (94)$$

where

$$H_{ij} = \frac{\Lambda_j M_i \exp(-\Lambda_j M_i \xi)}{\int_0^1 \exp(-\Lambda_j M_i \xi)\, dx}. \qquad (95)$$

Again a series of M_i are chosen using the procedures described previously, and the f_i for each series are obtained by linear programming. A data table of $V(\Lambda, \xi)$ for different choices of ξ and Λ is set up in the same manner as for sector-shaped centerpieces (see table 2 of ref. [27]). Fig. 14 shows our results using corrected (using the first approximation only) and uncorrected data; the manufacturer's MWD is shown here also. These results were obtained with Lot 7981.

4.4. MWDs from sedimentation velocity experiments

Since the weight average sedimentation coefficient, s_w, was determined from the second moment of the moving boundary curve, using Webber's [52] method, the same experimental data can also be used to evaluate $g^0(s_0)$, the differential distribution of sedimentation coefficients. If a relationship of the type $s_0 = K M_w^{\alpha}$ is available, then it is a simple matter to transform $g^0(s_0)$ to $f(M)$. Here we have followed procedures developed

by Baldwin and Williams [5,6c,23,36,37,57–60]; the procedures required for obtaining $g^0(s_0)$ from sedimentation velocity experiments have been quite elegantly described by Williams [38] in his recent monograph.

In order to obtain $g^0(s_0)$ it is first necessary to define an apparent differential distribution of sedimentation coefficients, $g^*(s)$, since both sedimentation and diffusion occur in the moving boundary. Here $g^*(s)$ is defined by [5,6c,23,36,37,57–60]

$$g^*(s) = \frac{1}{c_0}\left(\frac{r}{r_m}\right)^2\left(\frac{dc}{dr}\right)r\omega^2 t. \tag{96}$$

For each value of $g^*(s)$ we calculate an apparent value of s; this is done for each frame on the photographic plates. The apparent s values are obtained from the relation

$$s = \ln(r/r_m)/\omega^2 t. \tag{97}$$

The next step is to eliminate the effect of diffusion. Since the values of $g^*(s)$ and its corresponding s will be different at different times, we choose a set of different values of s and find the $g^*(s)$ corresponding to it at various times. These values of $g^*(s)$ are plotted against $1/t$ to infinite time ($1/t = 0$) to remove the effects of diffusion. This must be done for each initial concentration, c_0, used in these experiments. The values of $g^*(s)$ at $1/t = 0$ are denoted by $g^0(s)$.

In order to complete the analysis it is necessary to eliminate the concentration dependence of s and obtain the values of s at infinite dilution; these values of s are denoted as s_0. The concentration dependence of s can be represented by [6,60]

$$s = s_0/(1 + k_s c_0) \tag{98}$$

A plot of $1/s$ vs c_0 will have $1/s_0$ as an intercept and k_s/s_0 as a slope; k_s is the concentration dependence parameter of the sedimentation coefficient. Finally each $g^0(s)/g^0_{max}(s)$ is multiplied by $g^0_{max}(s)$ to give $g^0(s)$. These values of $g^0(s)$ are plotted against s_0 to obtain the true $g^0(s_0)$ vs s_0 curve. Several values of $g^0(s)$ vs s are plotted in fig. 15a; the curve we have marked $c_0 = 0$ is the true $g^0(s_0)$ curve.

In order to convert $g^0(s_0)$ to $f(M)$ it is necessary to have a relation of the type

$$s_0 = KM_w^{\alpha}. \tag{99}$$

Here we used data from Granath's [39] paper to obtain the required relation. Granath [39] has published data relating s and $[\eta]$ to M_w for dextrans produced by two strains of *Leuconostoc mesenteroides*. Our material was obtained from strain B512; some of Granath's material was obtained from this same strain. The values of K and α used here were $K = 2.24 \times 10^{-15}$ and $\alpha = 0.46$. These values were obtained by a least squares analysis of Granath's data. Fig. 16 shows the MWD obtained from the plot of $g^0(s_0)$ vs s_0. The manufacturer's MWD for lot 693 is shown by the curve with the solid line. Our plot indicates that a unimodal distribution is present, but our plot does not agree with the

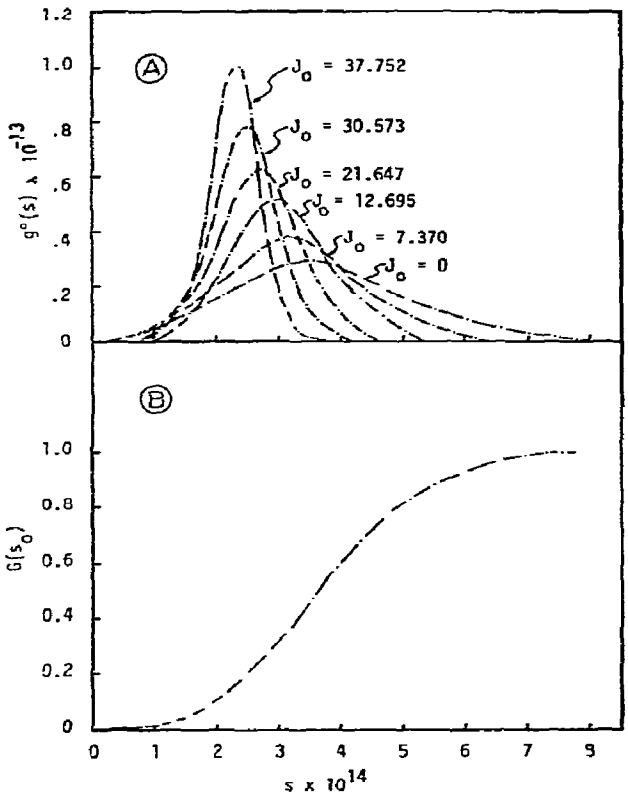

Fig. 15. Distribution of sedimentation coefficients. Lot 7981. (a) Differential distribution. Here values of $g^0(s)$ at infinite time are plotted against J_0, the initial concentration in fringes. The curve labelled $J_0 = 0$ is the true differential distribution of sedimentation coefficients, since the concentration dependence of the sedimentation coefficient has been eliminated. (b) Integral distribution. This curve is obtained by numerical integration of the plot of $g^0(s_0)$ vs s_0 (the plot in fig. 15a labelled $J_0 = 0$).

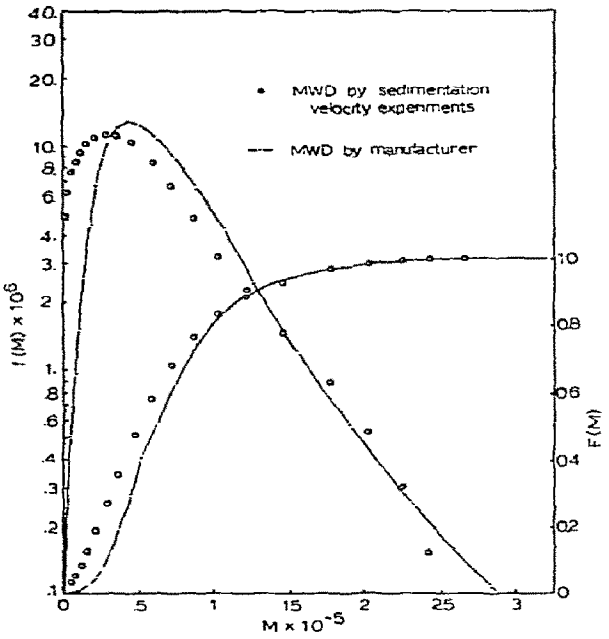

Fig. 16. MWD from sedimentation velocity experiments. Lot 7981. The $g_0^0(s_0)$ curve (see the plot labelled $J_0 = 0$ in fig. 15) can be converted to a differential MWD, $f(M)$, curve, if a relation $s = KM^{\alpha}$ exists. Using values of K and α obtained from Granath's [39] work, we were able to obtain these plots of the differential, $f(M)$, and integral, $F(M)$, MWDs. The manufacturer's differential and integral MWDs (dashed line) are also shown here.

manufacturer's MWD or the MWDs obtained from sedimentation equilibrium experiments. A plot of the integral distribution of sedimentation coefficients, $G(s_0)$, is also shown in fig. 15b; here

$$G(s_0) = \int_0^{s_0} g^0(s_0)\, ds_0. \qquad (100)$$

5. Discussion

We have reported here on various physical studies, mainly ultracentrifugal, on some dextran solutions. The values of M_n, M_w and M_z have been obtained independent of any knowledge of the MWD. These quantities can be used to help check the MWDs obtained by ultracentrifugation, since the experimental values of M_n, M_w and M_z can be compared with the corresponding values calculated from the MWD. This is not a perfect check, since there may be several distributions which can have the same values of M_n, M_w and M_z [5,6a]; nevertheless, it is conforting to have available a limited check on the calculations.

It is interesting to note the excellent agreement between our values of M_n and M_w with those reported by the manufacturer, especially since different experimental methods were used in each case. For M_n we used membrane osmometry, whereas the manufacturer used end group analysis [20,39]. Our values of M_w were obtained from intrinsic viscosity, sedimentation velocity and sedimentation elquilibrium experiments; the manufacturer used light scattering to obtain M_w [20,39]. The agreement between the values of M_w obtained by sedimentation equilibrium experiments and the light scattering experiments is remarkable. The values of M_w obtained from $[\eta]$ and s_w are in good agreement with the values from light scattering and from sedimentation equilibrium experiments. However, it should be noted that the values of $[\eta]$ are the same for both batches of dextran, which would imply that both batches of dextran would have the same M_w. Yet the values of M_w obtained by the light scattering and the sedimentation equilibrium experiments for each batch are different. Thus it appears that these methods are more sensitive than is $[\eta]$ for measurement of M_w. We have shown [7] that in the limit as $\Lambda \to 0$ the values of $M_{w\ app}$ calculated from eqs. (18) or (24) converge to $M^0_{w\ app}$. The plots in fig. 5 and the values of M_w and B_{LS} reported in table 2 clearly support this observation. This is one advantage that the sedimentation equilibrium experiments at different speeds have – that there are at least two ways to obtain $M^0_{w\ app}$ and to use it to obtain M_w and B_{LS}. Each method can serve as an internal check on the other method. This is an advantage that is unique to the ultracentrifuge, and it is a point overlooked in previous experimental studies [18, 19] with nonideal solutions of nonassociating macromolecules. It is also possible to obtain M_z by at least two different methods [see eqs. (34) and (35)] using $M_{z\ cell\ app}$ or $M_{z\ cell\ vol\ app}$, since in the limit of zero speed these quantities converge to $M^0_{z\ app}$. A plot of $1/M^0_{z\ app}$ vs c_0 has $1/M_z$ as an intercept and B_{SZ} as a slope [see eq. (36)]. The value of M_z reported in table 2 is based on eq. (34) only.

We have shown that the Albright and Williams

method [18] can be applied to cells with nonsector-shaped centerpieces; data obtained with these centerpieces are displayed in figs. 3, 4, and 5. It has been demonstrated that $M^0_{w\ app}$ can be obtained by four methods [from values of $M^0_{w\ app}$ obtained from the values of $M_{w\ app}$ calculated from eqs. (18), (22), (40) and (46)]. The agreement between the plots of $1/M^0_{w\ app}$ vs c_0 (see fig. 4) for various methods and the values of M_w and B_{LS} obtained with both centerpieces is quite good (see table 2). For nonsector-shaped centerpieces the values of $M^0_{w\ app}$ (or $1/M^0_{w\ app}$) obtained by the application of eqs. (18) or (22) agree quite well with the values of $M^0_{w\ app}$ (or $1/M^0_{w\ app}$) obtained from experiments in which sector-shaped centerpieces were used. The values of $M^0_{w\ app}$ for nonsector-shaped centerpieces obtained from the use of eqs. (40) or (46) did not give as good agreement with the values of $M^0_{w\ app}$ using sector-shaped centerpieces.

The best way to obtain M_w in nonideal solutions from sedimentation equilibrium experiments is to use the Albright and Williams method [18], but it is also the most tedious method. Its virtue is that it provides a way out of the difficulties produced by the redistribution of the polymeric components in a centrifugal field. It also has the advantage that the same experimental data can be used to obtain MWDs in addition to the values of M_w, M_z and B_{LS}; we have shown the MWDs obtained from these experimental data in section four. We have shown some aspects of the two Fujita methods [15,16] that allow the evaluation of B_{LS} and also M_w from a series of sedimentation equilibrium experiments at two different speeds, if the speeds are low enough. For the application of the first [15] method [see eqs. (26) and (27)] it was found experimentally that if one plotted $1/(\Delta c/c_0)$ vs c_0 at constant Λ, then straight line plots, like those shown in fig. 3, were usually obtained. The limiting slope of the plots in fig. 3 is B'/Λ. Plots based on the second Fujita method [16] are shown in fig. 5; the limiting slope of the plots of $1/(\Delta c/c_0)$ vs $\bar{c}$ at constant Λ is B^*/Λ. The results obtained by these modifications of the two Fujita methods show excellent agreement with the values of B_{LS} and M_w (see table 4) obtained by more thorough experiments. Attempts to evaluate α or β, the speed-dependent terms of the sedimentation equilibrium second virial coefficients (the B' or B^*), by these methods gave variable results (see table 4). The main disadvantage of the Fujita method is to find a low enough speed for the particular polymer sample being studied. For an unknown material this is a trial and error procedure. It is clear from this work (see table 4) that at higher speeds the complications from solute redistribution set in. It is possible to obtain the speed-dependent terms of the B' or B^*. First B' or B^* are evaluated from the limiting slopes of plots B' or B^* vs $\bar{c}$ (for B^*). Then one plots B' or B^* vs Λ^2. The slope of this plot is αB_{LS} when B' is used and βB_{LS} when B^* is used. Fig. 6 shows such plots; linear regression analysis was used to obtain the straight lines through the experimental points. The dashed line indicates the value of the slope predicted for the B' plot using the Fujita [15] assumption that all the B'_{ik} are equal The values of B_{LS}, α and β obtained from these plots are listed in table 2. It is evident from the plots shown in fig. 6 that all the B'_{ik} are not the same for all the polymeric solutes. This was also evident from the fact that there was a speed effect (see fig. 10) in the MWD of lot 7981, obtained by Donnelly's method, when eq. (50) was used to correct the data for nonideality.

The advantage of using a modulatable laser as a light source is that it allows one to perform several sedimentation equilibrium experiments in the same time that it takes to perform one run. With a four-hole rotor, it is possible to do 3 to 9 experiments, and with a six hole rotor it is possible to do 5 to 15 experiments. One hole must be reserved for the counterbalance; to do the larger number of experiments a multichannel, equilibrium centerpiece must be used. Automatic plate readers have been developed [61,62] and are available commercially (from Gaertner Instruments, Inc.). Not only will this take the tedium out of plate reading, but it should also allow for better precision, since one can take advantage of multiple scans and computer averaging.

Experimentally, we have found Donnelly's [7,24,25] method was easier to apply than was Scholte's [7,26–28 method. When corrections for nonideal behavior were applied, Donnelly's method gave quite good agreement with the manufacturer's MWD (obtained by a combination of analytical gel chromatography and light scattering). If our first model for the nonideal correction [see eq. (50)] were correct, then there would be no differences in the MWD obtained at various speeds, but fig. 10 showed that this was not the case.

The first model [see eq. (50)] that we used to correct for nonideality is somewhat similar to a model proposed by Schulz [5,63] and by Wales, Bender, Williams

and Ewart [5,9]. They assumed that $\ln y_i$ (y_i being the activity coefficient of solute component i) could be expressed as

$$\ln y_i = BM_i c,$$

where $c = \Sigma_i c_i$. It was assumed that the quantity B did not depend on the molecular weight of the polymer, but that it did depend on the temperature and on the polymer-solvent system used. Thus B could be evaluated from the concentration dependence of osmotic pressure or light scattering experiments. With this assumption it can be shown that

$$\frac{1}{M_{wr\ app}} = \frac{1}{M_{wr}} + Bc.$$

At the time these assumptions were made, it was not realized that the osmotic pressure (B_{OS}) and light scattering (B_{LS}) second virial coefficients were different [6b,18]. For homogeneous, nonassociating solutes $B_{LS} = 2B_{OS}$, but as Albright and Williams [18] have pointed out, this relation does not necessarily apply for heterogeneous, nonassociating solutes. Our first model, which assumes $\langle B'_{ik}\rangle_r \approx B_{LS}$, would be exact when all the B'_{ik} are equal, and under these circumstances it would become identical to the Schulz [63] and the Wales, Bender et al. [9] method. We have approached our first assumption from a more recent point of view, since $\ln y_i$ is described by eq. (A.3) and eq. (A.9) shows that $\lim_{\Lambda\to 0} \langle B'_{ik}\rangle_r = B_{LS}$.

It is evident from figs. 6, 9 and 10, and also from table 2, that the B_{LS} term is the largest contribution to the nonideal behavior, since the speed-dependent terms, the α and β, are much smaller in magnitude. It is tempting to use the manufacturer's MWD as a standard for comparison since Granath and her associates [20,39,40] did such careful, elegant work, yet one must remember that their MWDs are also subject to error. The fact that there is a slight speed-dependence of the MWDs in fig. 10 suggests that an additional correction is needed, but which correction, the second or third approximation [see eqs. (51) or (52)], is better? Also, one must remember that α and β are limiting values, since they are obtained from the limiting slope of plots of B' or B^* vs Λ^2. Additional speed-dependent terms have not been obtained, so as the speed increases $\alpha\Lambda^2$ and $\beta\Lambda^2$ will become larger; thus the use of $\alpha\Lambda^2$ and $\beta\Lambda^2$ appears to be restricted to experiments at lower speeds unless other (presently unavailable) compensatory speed-dependent terms are included. It is evident from fig. 11, which shows the effect of the second and third methods for nonideal correction at various speeds, that there are very small differences in the corrected MWDs. If we were able to obtain an MWD under ideal, dilute solution conditions, then we could make a comparison of the ideal MWD and the corrected MWD. If this ideal MWD is unavailable, then the best that one can do is to compare independently determined values of various average molecular weights (M_n, M_w and M_z) with those calculated from the corrected MWDs. Table 6 shows values of M_n, M_w and M_z obtained at various speeds for the three methods of estimating $\langle B'_{ik}\rangle_r$; the results at 6000 RPM also include values of M_n, M_w and M_z obtained for our estimates of $\langle B'_{ik}\rangle$ at $u = 1/2$ and at $c = \bar{c}$. The values of M_n, M_w and M_z estimated from the manufacturer's MWD are also shown in this table. It is apparent from this table that as the speed increases, the values of M_n and M_z decrease, whereas the value of M_w tends to increase. It acts as if the MWD were sharpening and converging towards M_w. Both the second and third methods for nonideal correction seem to give better overall agreement with the independently determined values of M_n, M_w and M_z than do the other methods of nonideal corrections, with the second method having a slight edge. All methods for nonideal correction seem to work best at the lowest speed.

Unfortunately, we did not obtain particularly good results with Scholte's [7,26–28] method. When we tried to use the data obtained at seven speeds with lot 693, we got peculiar results; sometimes we would get a spike in the MWD at very low molecular weights. Our speeds were chosen so that the values of Λ would differ by a factor of 2. Even so, with lot 693 we were only able to use three of the seven speeds to obtain a resemblance to the unimodal MWD encountered by other physical methods. Thus, this procedure gave only a few values of $f(M)$ and M, and this limited data (see fig. 13) only suggests the trend of the MWD. One might be able to draw several MWDs through these data points. Fig. 14 shows results obtained with nonsector-shaped centerpieces with lot 7981; four speeds were used here. While these data look somewhat better, we still encountered a paucity of values of $f(M)$ and M. Fig. 4 of the preliminary communication [1] shows results obtained with lot 7981 using sector- and non-sector-shaped centerpieces. Because of the higher speeds required by Scholte's

Table 6
Dextran T-70 Lot 693

A. Values of M_n, M_w, M_z and M_{z+1} calculated from MWDs obtained by Donnelly's method [24,25] before and after correction for nonideal behavior

Condition	Speed (RPM)	$M_n \times 10^{-4}$	$M_w \times 10^{-4}$	$M_z \times 10^{-4}$	$M_{z+1} \times 10^{-4}$
No correction	4400	3.38	4.42	5.47	6.53
	6000	3.58	4.39	5.24	6.08
	8000	3.58	4.22	4.80	5.40
	10000	3.35	4.02	4.54	5.11
Corrected by method I, eq. (50)	4400	2.48	6.54	9.49	12.95
	6000	2.44	6.68	8.93	12.14
	8000	2.21	6.68	7.98	10.81
	10000	1.83	6.93	7.47	10.21
Corrected by method II, eq. (51)	4400	2.48	6.55	9.51	12.98
	6000	2.42	6.72	8.99	12.24
	8000	2.16	6.84	8.15	11.11
	10000	1.69	7.50	7.91	10.96
Corrected by method III, eq. (52)	4400	2.48	6.55	9.49	12.96
	6000	2.43	6.69	8.95	12.17
	8000	2.19	6.73	8.04	10.91
	10000	1.79	7.11	7.61	10.45
Corrected by method IV, eq. (53)	4400	2.40	6.77	9.88	13.57
	6000	2.04	7.96	10.64	14.86
Corrected by method V, eq. (A.31)	4400	2.60	6.20	8.88	11.98
	6000	2.82	5.75	7.54	9.83

B. Values of M_n, M_w, M_z and M_{z+1} estimated from the Pharmacia MWD

	Lot 693	Lot 7981
$M_n \times 10^{-4}$	3.96	4.93
$M_w \times 10^{-4}$	6.75	7.18
$M_z \times 10^{-4}$	10.61	9.81
$M_{z+1} \times 10^{-4}$	14.22	12.74

The unit for the average molecular weights is the dalton.

[26–28] method, only the first method for nonideal correction [see eq. (50)] was used. It may be that Scholte's method is better suited for samples having a broader MWD. We have found that the choice of molecular weights for the first series or grid of molecular weights influences the results considerably. While the MWDs obtained with Donnelly's method or the MWD provided by the manufacturer suggest the molecular

weight range to be covered, there is no clear cut guide on how to choose the first series of molecular weights. Part of our difficulties with Scholte's [26–28] method may arise from the fact that we are dealing with nonideal solutions, and it is more difficult to make a good estimate of c_{id} or $[dc/d(r^2)]_{id}$ at the higher speeds used in Scholte's [26–28] method. Heretofore, his method has been restricted to ideal, dilute solutions. Some similar difficulties with Scholte's method have been encountered by Gehatia and Wiff (personal communication); in fact this led them to develop their own method for MWDs from sedimentation equilibrium experiments.

For multimodal distributions Scholte's [26–28] or the Gehatia and Wiff [31–36] methods are the methods of choice. We elected to use Scholte's [26–28] method because we were more familiar with it and thought that we understood it better than we did the Gehatia and Wiff [31–36] method. Scholte [28] has shown that he can detect a trimodal blend of polystyrene fractions dissolved in cyclohexane at 35°C by sedimentation velocity or sedimentation equilibrium experiments. The MWDs from the ultracentrifugal methods and from analytical gel chromatography on the same sample were trimodal, yet each MWD differed in shape from each other.

For unimodal distributions Donnelly's [24,25] method is quite good. With a set of sedimentation equilibrium experiments at two speeds, one can make an estimate of B_{LS} (see table 4). M_z can also be estimated from two sets of experiments. With three speeds one should be able to get a fair estimate of α and β also.

The MWD from sedimentation velocity experiments also gave a unimodal MWD; however, this MWD did not agree as well with the manufacturer's MWD as did the MWDs obtained from corrected sedimentation equilibrium data. This may be due to the fact that two extrapolations are required – one to infinite time to eliminate the effects of diffusion, and then a second extrapolation (using the data at infinite time) to zero concentration to eliminate the concentration dependence of the sedimentation coefficient [5,37,38]. With organic solvents an additional extrapolation to eliminate pressure effects is required [60,64], but the very small isothermal compressibility of water means that this correction is negligible. Attempts to measure pressure effects on the partial specific volume of the solute or on its sedimentation coefficient in aqueous solutions have shown that these effects are negligible [65,66]. The discrepancy in the MWD could be due to the extrapolation required by the method, or it could be due to the choice of K and α in eq. (99). Ideally, one should have had a series of dextran samples which had been hydrolyzed from the same lot; since this was not the case, we had to assume that the properties of the dextran samples used by Granath [39] applied to our sample as well. With a slightly branched polymer like dextran, this assumption might be risky; however, Scholte [28] has noted differences in the MWD obtained by sedimentation velocity experiments and by other methods.

Three statistical distribution functions were used to examine the MWD of one dextran sample (lot 693). They are the Schulz, the logarithmic normal and the most probable distributions [6e,67]. The values of M_n and M_w obtained from osmotic pressure and sedimentation equilibrium experiments (see table 2), respectively, were used to calculate the two parameters needed for these distributions. Fig. 17 shows the three differential MWDs together with the manufacturer's MWD for lot 693. Apparently the Schulz distribution function describes the MWD of the dextran sample (lot 693) best. The virtue of Donnelly's [24,25] or Scholte's [26–28] methods is that one does not have to prejudge the MWD, whereas the application of a statistical distribution function only, like the functions mentioned above, implies that one has prejudged the distribution.

Since both dextran samples (lot # 7981 and 693) covered about the same molecular weight range, but had differences in their MWDs, we wondered what would happen if we used the nonideal correction obtained with one batch to correct the sedimentation equilibrium data for the other batch? Thus we applied the B_{LS} obtained from lot 7981 to the correction of sedimentation equilibrium data obtained with lot 693. The results using this first method for nonideal correction are shown in fig. 18; corrected and uncorrected data are shown along with the manufacturer's MWD (dashed line). This may have important practical considerations. It indicates that if careful studies are done on the MWD of a standard sample, the nonideal corrections can be applied to samples having a similar MWD so that a good estimate of the correct MWD can be made. This could be significant in the quality control of commercially important polymers or biopolymers.

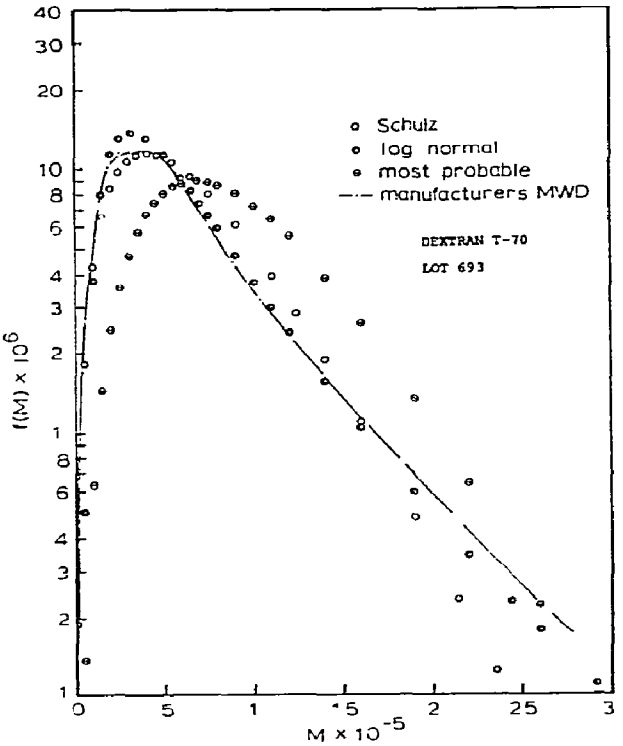

Fig. 17. Comparison of three statistical MWDs with the manufacturer's MWD. Lot 693. Values of M_n and M_w were used to calculate the two parameters which are needed so that the Schulz, the log normal, and the most probable [6e,67] MWDs could be obtained. Only the differential MWD is shown here. The Schulz distribution seems to describe the manufacturer's MWD (dashed line) best. This was also true with lot 7981.

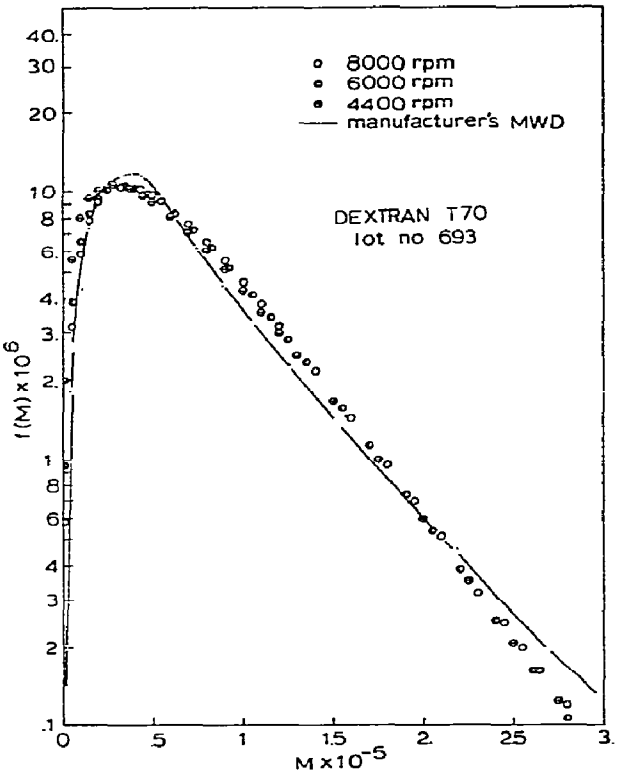

Fig. 18. Corrected MWD for lot 693. Donnelly's method [24, 25]. Sector-shaped centerpiece. Method I [see eq. (50)] was used to correct the sedimentation equilibrium data. We used the value of B_{LS} obtained with lot 7981 to correct the sedimentation equilibrium data obtained with lot 693. Note the good agreement with the manufacturer's MWD (dashed line). Also note the difference between this figure and fig. 10a.

Fig. 18 also indicates that any further nonideal correction for lot 693, beyond the B_{LS} for this lot, would be a very small correction.

In conclusion we have shown how one can use sedimentation equilibrium experiments to evaluate the M_w and M_z of a polymeric solute, as well as obtain various nonideal terms ($B_{LS}, B_{SZ}, \alpha, \beta$) from these experiments. These quantities can be used to correct sedimentation equilibrium data, so that a corrected or quasi-ideal MWD can be obtained. Several methods for correcting the nonideal behavior have been shown and the limitations of the various methods have been discussed. We have also shown that the data required for the evaluation of s_w can also be used to obtain $g^0(s_0)$, which can then be converted to a MWD. Both ultracentrifugal methods gave unimodal distributions, but the sedimentation equilibrium MWD gives better agreement with the manufacturer's MWD. The theory for MWDs from sedimentation equilibrium experiments is more rigorous, but the experiments take much longer to perform than do sedimentation velocity experiments. The ideal way to correct sedimentation equilibrium experiments for nonideal behavior would be know or have an estimate of the values of $\langle B'_{ik}\rangle_r$ at each $r(r_m \leqslant r \leqslant r_b)$. When we began these studies, this seemed to be a virtual impossibility, and we chose the first three methods to simulate $\langle B'_{ik}\rangle_r$. Now it may be possible to make an estimate of the $\langle B'_{ik}\rangle_r$ at each r, provided the speed is low so that $\Lambda M_i < 2\pi$. We can use methods developed for estimating $\langle B'_{ik}\rangle_{\bar{c}}$ (see appendix A.4) to develop ex-

pressions for the $\langle B'_{ik}\rangle_r$ at various values of r; in appendix A.5 we have indicated how this might be done at $u = 0$, 1/2 and 1. Clearly, if this can be done, then we can make estimates of $\langle B'_{ik}\rangle_r$ at other values of u. At present it appears that these methods are limited to low speeds (less than 8000 RPM for our experiments) and sector-shaped centerpieces. It is not known now how many terms will be needed in the series expansions of the $\langle B'_{ik}\rangle_r$ or how critically we have to know values of M_z, M_{z+1}, α and B_{SZ}, or whether we will be able to estimate the additional higher terms that would appear in the numerator of the various equations for the $\langle B'_{ik}\rangle_r$. The additional terms in the denominator of these equations can be estimated from a prior estimate of the MWD. We hope to report further on this matter and also on other ways to obtain MWDs from sedimentation equilibrium experiments.

Acknowledgement

We are very grateful to the National Science Foundation for their support of this work through grants GB32242 and BMS72-01873. Many thanks are due to Dr. Th. G. Scholte for sending us a copy of his computer program.

Appendix

A.1. The basic sedimentation equilibrium equation

At constant temperature the basic sedimentation equilibrium equation for nonideal associating solutes is [6b,7,17,18]

$$-\Lambda M_i c_{ir} = dc_{ir}/d\xi + M_i c_{ir} \sum_k (dc_{kr}/d\xi)\, B'_{ik}, \qquad (A.1)$$

where for solute concentrations in g/ℓ [7]

$$B'_{ik} = B_{ik} + \bar{v}/1000\, M_k. \qquad (A.2)$$

The quantities B_{ik} are nonideal terms which are related to the activity coefficient, y_i, of solute component i through a relation of the type

$$\ln y_i = M_i \sum_k B_{ik} c_k. \qquad (A.3)$$

For simplicity we will drop the subscript r, so that c_i, c_k or will refer to concentrations at any radial position $r(r_m \leqslant r \leqslant r_b)$. If we assume as others have done [7,17,18] that in the nonideal term in eq. (A.1) that

$$dc_k/d\xi = -\Lambda M_k c_k, \qquad (A.4)$$

then after the substitution of eq. (A.4) into eq. (A.1), one obtains

$$-\Lambda M_i c_i = dc_i/d\xi - \Lambda c_i M_i \sum_k B'_{ik} c_k M_k. \qquad (A.5)$$

Summation over the i solute components leads to

$$-\Lambda c M_{wr} = dc/d\xi - \Lambda \langle B'_{ik}\rangle_r (cM_{wr})^2. \qquad (A.6)$$

Here,

$$\langle B'_{ik}\rangle_r = \frac{\Sigma_i \Sigma_k c_i c_k M_i M_k B'_{ik}}{\Sigma_i \Sigma_k c_i c_k M_i M_k}. \qquad (A.7)$$

Equation (A.6) can be rearranged to give

$$-\frac{1}{\Lambda c}\frac{dc}{d\xi} = M_{wr\,app} = \frac{M_{wr}}{1 + \langle B'_{ik}\rangle_r cM_{wr}}, \qquad (A.8)$$

where

$$M_{wr} = \sum_i c_{ir} M_i / c_r.$$

Eq. (A.6) or (A.8) are the basic sedimentation equilibrium equations.

A.2. The analog of Fujita's 1969 method

As $\Lambda \to 0$, $c_i \to c_i^0$ and $c_k \to c_k^0$ (the initial concentrations of component i and k), so that

$$B_{LS} = \lim_{\Lambda \to 0} \langle B'_{ik}\rangle_r = \frac{\Sigma_i \Sigma_k f_i f_k M_i M_k B'_{ik}}{\Sigma_i \Sigma_k f_i f_k M_i M_k}, \qquad (A.9)$$

$$f_j = c_j^0/c_0 \qquad (j = i \text{ or } k).$$

This suggests that as a first approximation one might replace $\langle B'_{ik}\rangle_r$ by B_{LS}. When this is done eq. (A.6) becomes

$$-\Lambda c M_{wr} = dc/d\xi - \Lambda B_{LS} (cM_{wr})^2 + \ldots. \qquad (A.10)$$

Using the assumption in the nonideal terms that $dc/d\xi \approx -\Lambda c M_{wr}$, one obtains

$$\frac{dc}{d\xi} + B_{LS} c M_{wr} \frac{dc}{d\xi} + \ldots = -\Lambda c M_{wr}. \quad (A.11)$$

Let us define $u = (r^2 - r_m^2)/(r_b^2 - r_m^2)$. It follows that $u = 1 - \xi$, since $\xi = (r_b^2 - r^2)/(r_b^2 - r_m^2)$; it also follows that $du/d\xi = -1$ and that $dc/d\xi = -dc/du$.

$$\frac{dc}{du} + B_{LS} c M_{wr} \frac{dc}{du} + \ldots = -\Lambda c M_{wr}. \quad (A.12)$$

Eq. (A.12) is an analog of Fujita's [16] eq. (8). The only difference is that we use B_{LS} and Fujita [16] uses B. He assumes that all the B'_{ik} are the same for each polymeric component, whereas we avoid this assumption. If the B'_{ik} are all the same, then $B = B_{LS}$. Our eq. (A.12) can be used in the Fujita [16] procedure to obtain

$$\frac{1}{M_{w\ cell\ app}} = \frac{1}{M_w} + B^* \bar{c}, \quad (A.13)$$

where $B^* = B_{LS}(1 + \Delta)$. When solute concentrations in g/ℓ are used, the values of B^* [and also B' – see eq. (28)] will be 1000 times smaller than their values would be if the solute concentration unit were gm/ml.

A.3. Derivation of the equations for $M_{z\ cell\ app}$ and $1/M_{z\ cell\ app}$

Eq. (A.6) can be rearranged to give

$$\frac{1}{\Lambda}\frac{dc}{du} = cM_{wr\ app} = cM_{wr} - \sum_i \sum_k c_i c_k M_i M_k B'_{ik} \quad (A.14)$$

The quantity $M_{zr\ app}$ is defined by

$$M_{zr\ app} = d(cM_{wr\ app})/dc$$

$$= M_{zr} - \sum_i \sum_k M_i M_k B'_{ik} \left(c_k \frac{dc_i}{dc} + c_i \frac{dc_k}{dc} \right). \quad (A.15)$$

If we assume in the nonideal term in eq. (A.15) that

$$\frac{dc_j}{dc} = \left(\frac{dc_j}{du}\right) \Big/ \left(\frac{dc}{du}\right) \approx \frac{\Lambda c_j M_j}{\Lambda c M_{wr}} = \frac{c_j M_j}{cM_{wr}}, \quad (A.16)$$

($j = i$ or k), then eq. (A.15) becomes

$$M_{zr\ app} = M_{zr} - \sum_i \sum_k \frac{c_i c_k M_i M_k B'_{ik} (M_i + M_k)}{cM_{wr}}. \quad (A.17)$$

The quantity $M_{z\ cell\ app}$ is defined by

$$M_{z\ cell\ app} = \int_{c_m}^{c_b} M_{zr\ app}\, dc \Big/ \int_{c_m}^{c_b} dc. \quad (A.18)$$

In order to obtain an equation for $M_{z\ cell\ app}$, not only must one substitute eq. (A.16) into eq. (A.15), but the following relations must also be used:

$$dc \approx \Lambda c M_{wr} du,$$

$$\Delta c = \int_{c_m}^{c_b} dc = \Lambda c_0 M_{w\ cell\ app},$$

and it is assumed that c_j ($j = i$ or k) can be represented by [7,13,68]

$$c_j = \frac{\Lambda M_j c_j^0 \exp(-\Lambda M_j \xi)}{1 - \exp(-\Lambda M_j)} = \frac{\Lambda M_j c_j^0 \exp(\Lambda M_j u)}{\exp(\Lambda M_j) - 1}$$

$$= c_j^0 \left\{ 1 + \Lambda M_j \left(u - \frac{1}{2} \right) + \Lambda^2 M_j^2 \left(\frac{u^2}{2} - \frac{u}{2} + \frac{1}{12} \right) + \Lambda^3 M_j^3 \left(\frac{u^3}{6} - \frac{u^2}{4} + \frac{u}{12} \right) + \ldots \right\}, \quad (A.19)$$

if $|\Lambda M_j| < 2\pi$. Here $u = 1 - \xi$. Using these relations, eq. (A.18) becomes

$$M_{z\ cell\ app} = M'_{z\ cell} - \frac{1}{\Lambda c_0 M_{w\ cell\ app}} \times \left\{ \sum_i \sum_k \int_0^1 M_i^2 M_k^2 B'_{ik} c_i^0 c_j^0 \Lambda^3 (M_i + M_k) \times \exp[\Lambda (M_i + M_k)]\, u\, du \Big/ (\exp(\Lambda M_i) - 1)(\exp(\Lambda M_j) - 1) \right\}. \quad (A.20)$$

If we use the Laurent series expansion for $\Lambda M_j/[\exp(\Lambda M_j) - 1]$, then we obtain

$$\frac{\Lambda M_j}{\exp(\Lambda M_j) - 1} = 1 - \frac{\Lambda M_j}{2} + \frac{(\Lambda M_j)^2}{12} - \frac{(\Lambda M_j)^4}{720} + \ldots, \quad (A.21)$$

for $|\Lambda M_j| < 2\pi$. If we also expand $\exp(\Lambda M_j)$ in its power series, and then multiply this series and the Laurent series, we obtain

$$M_{z\,\text{cell app}} = M_{z\,\text{cell}} - \frac{c_0}{M_{wa}}\left(\sum_i\sum_k f_i f_k M_i M_k (M_i + M_k) \times B'_{ik}\,(1 + \tfrac{1}{12}\Lambda^2 M_i M_k + O(\Lambda^4) + \ldots)\right)$$

$$= M_{z\,\text{cell}} - \frac{c_0}{M_{w\,\text{app}}}\left(\sum_i\sum_k f_i f_k M_i M_k (M_i + M_k) B'_{ik}\,(1 + \gamma\Lambda^2)\right). \qquad \text{(A.22)}$$

Here γ is defined by eq. (38). Now take the reciprocal of $M_{z\,\text{cell app}}$ to obtain

$$\frac{1}{M_{z\,\text{cell app}}} = \frac{1}{M_z} + \frac{c_0\,[1 + (B_{LS} + \alpha\Lambda^2)\,c_0 M_w]}{M_w M_z^2} \times \left(\sum_i\sum_k f_i f_k M_i M_k (M_i + M_k) B'_{ik}\,(1 + \gamma\Lambda^2) + \ldots\right)$$

$$\approx \frac{1}{M_z} + B_{SZ}\,c_0\,(1 + \gamma\Lambda^2) + \ldots . \qquad \text{(A.23)}$$

A.4. Evaluation of $\langle B'_{ik}\rangle_r$ at $\bar{c}$ (sector-shaped centerpiece)

The quantity $\langle B'_{ik}\rangle_r$ is defined by eq. (A.7); in this equation $c_j = c_{jr}$ ($j = i$ or k). The quantity $\bar{c}$ is defined by

$$\bar{c} = \tfrac{1}{2}(c_b + c_m) = \tfrac{1}{2}\sum_j [c_j(u=0) + c_j(u=1)] = \sum_j \bar{c}_j . \qquad \text{(A.24)}$$

If we assume that the Bernoulli polynomial expansion of c_j [see eq. (A.19)] can represent c_j, and if we insert $u = 0$ and $u = 1$ in the appropriate series, then we obtain

$$\bar{c}_j = c_j^0\,(1 + \tfrac{1}{12}\Lambda^2 M_j^2 + \ldots). \qquad \text{(A.25)}$$

Now let the value of $\langle B'_{ik}\rangle_r$ at the radial position where $c = \bar{c}$ be denoted by $\langle B'_{ik}\rangle_{\bar{c}}$, then

$$\langle B'_{ik}\rangle_{\bar{c}} = \frac{\Sigma_i\Sigma_k f_i f_k M_i M_k B'_{ik}\,[1 + \frac{1}{12}\Lambda^2 (M_i^2 + M_k^2) + \ldots]}{\Sigma_i\Sigma_k f_i f_k M_i M_k\,[1 + \frac{1}{12}\Lambda^2 (M_i^2 + M_k^2) + \ldots]}, \qquad \text{(A.26)}$$

since $c_j^0 = f_j c_0$ ($j = i$ or k).

The denominator of eq. (A.26) can be written as

$$M_w^2 + \tfrac{1}{12}\,2\Lambda^2 M_w^2 M_z M_{z+1} + \ldots = M_w^2\,(1 + \tfrac{1}{6}\Lambda^2 M_z M_{z+1} + \ldots) \qquad \text{(A.27)}$$

The numerator of eq. (A.26) can be written as

$$B_{LS} M_w^2 = \tfrac{1}{12}\Lambda^2 \sum_i\sum_k f_i f_k M_i M_k (M_i^2 + M_k^2) B'_{ik} + \ldots = B_{LS} M_w^2 \left(1 + \tfrac{1}{12}\Lambda^2 \frac{\Sigma_i\Sigma_k f_i f_k M_i M_k (M_i^2 + M_k^2) B'_{ik}}{\Sigma_i\Sigma_k f_i f_k M_i M_k B'_{ik}} + \ldots\right). \qquad \text{(A.28)}$$

We do not know the value of $F = \Sigma_i\Sigma_k f_i f_k M_i M_k (M_i^2 + M_k^2) B'_{ik}$, nor do we have a way to measure it directly. One can use eqs. (27) and (38) to show that

$$24\alpha B_{LS} M_w^2 < F < 12 B_{SZ} M_w M_z^2 .$$

Here

$$2\sum_i\sum_k f_i f_k M_i^2 M_k^2 B'_{ik} = 24\alpha' B_{LS} M_w^2,$$

and

$$\sum_i\sum_k f_i f_k M_i^2 M_k^2 (M_i + M_k) B'_{ik} = 12\gamma B_{SZ} M_w M_z^2 .$$

Thus we do know the range of values that F could have. The simplest procedure is to assume that

$$\frac{\Sigma_i\Sigma_k f_i f_k M_i M_k (M_i^2 + M_k^2) B'_{ik}}{2\Sigma_i\Sigma_k f_i f_k M_i^2 M_k^2 B'_{ik}} \approx \frac{M_{z+1}}{M_z} \qquad \text{(A.29)}$$

Since this is the value that this fraction would have if all the B'_{ik} are equal. So, as a first approximation, it is assumed that

$$\sum_i \sum_k f_i f_k M_i M_k (M_i^2 + M_k^2) B'_{ik} \approx 24\alpha' B_{LS} M_w^2 (M_{z+1}/M_z), \quad \text{(A.30)}$$

and hence

$$\langle B'_{ik} \rangle_{\bar{c}} \approx \frac{B_{LS}(1 + 2\alpha'(M_{z+1}/M_z)\Lambda^2 + \ldots)}{1 + \frac{1}{6}\Lambda^2 M_z M_{z+1} + \ldots}. \quad \text{(A.31)}$$

A.5. Evaluation of $\langle B'_{ik} \rangle_r$ at $u = 0$, $u = 1/2$ and $u = 1$ (sector-shaped centerpieces)

We can use the procedures similar to thos employed in appendix A.4 to obtain estimates of the $\langle B'_{ik} \rangle_r$ at various radial positions. The results will be illustrated with three examples – the values of $\langle B'_{ik} \rangle_r$ at $u = 0$, $u = 1/2$ and $u = 1$. In order to obtain these results we will have to assume that eq. (A.29) is valid and that eq. (A.19) can be used for estimating $c_j(u)$.

At $u = 0$

$$c_j(u = 0) = c_j^0 (1 - \tfrac{1}{2}\Lambda M_j + \tfrac{1}{12}\Lambda^2 M_j^2 + 0 + \ldots), \quad \text{(A.32)}$$

and

$$\langle B'_{ik} \rangle_{(u=0)} = \frac{B_{LS}\left(1 - \dfrac{\Lambda B_{SZ} M_z^2}{2B_{LS} M_w} + [3 + 2(M_{z+1}/M_z)]\,\alpha'\Lambda^2 + \ldots\right)}{1 - \Lambda M_z + \frac{1}{12}\Lambda^2 (3M_z^2 + 2M_z M_{z+1}) + \ldots} \quad \text{(A.33)}$$

At $u = 1/2$

$$c_j(u = 1/2) = c_j^0 (1 - \tfrac{1}{24}\Lambda^2 M_j^2 + \ldots), \quad \text{(A.34)}$$

and

$$\langle B'_{ik} \rangle_{(u=1/2)} = \frac{B_{LS}[1 - \Lambda^2 (M_{z+1}/M_z)\alpha' + \ldots]}{1 - \frac{1}{12}\Lambda^2 M_z M_{z+1}}. \quad \text{(A.35)}$$

At $u = 1$

$$c_j(u = 1) = c_j^0 (1 + \tfrac{1}{2}\Lambda M_j + \tfrac{1}{12}\Lambda^2 M_j^2 + 0 \ldots), \quad \text{(A.36)}$$

and

$$\langle B'_{ik} \rangle_{(u=1)} = \frac{B_{LS}\left(1 + \dfrac{\Lambda B_{SZ} M_z^2}{2B_{LS} M_w} + \alpha'\Lambda^2 (3 + 2M_{z+1}/M_z) + \ldots\right)}{1 + \Lambda M_z + \frac{1}{12}\Lambda^2 (3M_z^2 + 2M_z M_{z+1}) + \ldots}. \quad \text{(A.37)}$$

It should be emphasized that the series expansions involved in obtaining eqs. (A.33), (A.35), and (A.37) are only valid for $|\Lambda M_j| < 2\pi$.

References

[1] Peter J. Wan and E.T. Adams, Jr., Polymer Preprints 15 (1974) 509.
[2] Theodor Svedberg and H. Rinde, J. Amer. Chem. Soc. 46 (1924) 2677.
[3] H. Rinde, Ph.D. Dissertation, University of Uppsala (1924).
[4] T. Svedberg and K.O. Pedersen, The Ultracentrifuge (Clarendon Press, Oxford, 1940); (a) pp. 342–353; (b) pp. 312–313.
[5] J.W. Williams, R.L. Baldwin, K.E. Van Holde and H. Fujita, Chem. Revs. 58 (1958) 715.
[6] H. Fujita, Mathematical Theory of Sedimentation Analysis (Academic Press, New York, 1960); (a) pp. 279–290; (b) pp. 263–279; (c) pp. 166–193; (d) p. 239 and p. 265; (e) pp. 296–297.
[7] E.T. Adams, Jr., P.J. Wan, D.A. Soucek and G.H. Barlow, Advan. Chem. Ser. No. 125 (1973) 235.
[8] W.D. Lansing and E.O. Kraemer, J. Amer. Chem. Soc. 57 (1935) 1369.
[9] M. Wales, M. Bender, J.W. Williams and R.H. Ewart, J. Chem. Phys. 14 (1946) 353.
[10] M. Wales, J. Phys. Colloid Chem. 52 (1948) 235.
[11] M. Wales, J. Phys. Colloid Chem. 55 (1951) 282.
[12] M. Wales, F.T. Adler and K.E. Van Holde, J. Phys. Colloid Chem. 55 (1951) 145.
[13] E.T. Adams, Jr., in: Characterization of Macromolecular Structure, Publication no. 1573 (National Academy of Sciences, Washington, D.C., 1968) p. 106.
[14] L. Mandelkern, L.C. Williams, and S.G. Weissberg, J. Phys. Chem. 61 (1957) 271.
[15] H. Fujita, J. Phys. Chem. 63 (1959) 1326.
[16] H. Fujita, J. Phys. Chem. 73 (1969) 1759.
[17] H.W. Osterhoudt and J.W. Williams, J. Phys. Chem. 69 (1965) 1050.
[18] D.A. Albright and J.W. Williams, J. Phys. Chem. 71 (1967) 2780.
[19] H. Utiyama, N. Tagata and M. Kurata, J. Phys. Chem. 73 (1969) 1448.

[20] Information sheet provided for each dextran sample by Pharmacia Fine Chemicals, Piscataway, New Jersey (see also the brochure, Dextran Fractions, Dextran Sulphate and DEAE-Dextran, Pharmacia Fine Chemicals, Uppsala, Sweden, 1971).
[21] Allene Jeanes, in: Encyclopedia of Polymer Science and Technology, eds. H.F. Mark, N.G. Gaylord and N.M. Bikales (Interscience, New York, 1966) Vol. 4, pp. 805–824.
[22] P.J. Baker, Jr. in Industrial Gums, eds. R.L. Whister and J.N. BeMiller (Academic Press, New York, 1959) pp. 531–563.
[23] J.W. Williams and W.M. Saunders, J. Phys. Chem. 58 (1954) 854.
[24] T.H. Donnelly, J. Phys. Chem. 70 (1966) 1862.
[25] T.H. Donnelly, Ann. N.Y. Acad. Sci. 164 (1969) 156.
[26] Th. G. Scholte, J. Polymer Sci. 164 (1969) 147.
[27] Th. G. Scholte, Ann. N. Y. Acad. Sci. 164 (1969) 156.
[28] Th. G. Scholte, Eur. Polymer J. 6 (1970) 51.
[29] S.W. Provencher, J. Chem. Phys. 46 (1967) 3229.
[30] L.-O. Sundelöf, Arkiv för Kemi 29 (1968) 297.
[31] M. Gehatia and D.R. Wiff, J. Polymer Sci. Part A–2, 8 (1970) 2039.
[32] M. Gehatia, Polymer Preprints 12 (1971) 875.
[33] M. Gehatia and D.R. Wiff, Eur. Polymer J. 8 (1972) 585.
[34] M. Gehatia and D.R. Wiff, J. Chem. Phys. 57 (1972) 1070.
[35] D.R. Wiff and M. Gehatia, J. Macromol. Sci. Phys. B6 (1972) 287.
[36] M. Gehatia and D.R. Wiff, Advan. Chem. Ser. No. 125 (1973) 216.
[37] J.W. Williams, W.M. Saunders and J.W. Cicirelli, J. Phys. Chem. 58 (1954) 774.
[38] J.W. Williams, Ultracentrifugation of Macromolecules: Modern Topics, (Academic Press, New York, 1972).
[39] K.A. Granath, J. Colloid Sci. 13 (1958) 308.
[40] K.A. Granath, Makromol. Chem. 28 (1958) 1.
[41] A. Kruis, Z. Phys. Chem. 34B (1936) 13.
[42] J. Brandrup and E.H. Immergut, eds., Polymer Handbook (Interscience, New York, 1966); (a) p. IV–302; (b) p. IV–111.
[43] K.E. Van Holde, Fractions, No. 1 (1967).
[44] C.H. Chervenka, A Manual of Methods for the Analytical Ultracentrifuge, Spinco Division of Beckman Instruments, Inc., Palo Alto, CA. (1969).
[45] J.M. Creeth and R.H. Pain, Prog. Biophys. Mol. Biol. 17 (1967) 217.
[46] F.W. Billmeyer, Jr., Textbook of Polymer Science, 2nd Ed. (Wiley–Interscience, New York, 1971); (a) pp. 84–90; (b) pp. 64–75.
[47] C. Tanford, Physical Chemistry of Macromolecules (Wiley, New York, 1961) p. 391.
[48] P.J. Flory, Principles of Polymer Chemistry (Cornell Univ. Press, Ithaca, New York, 1953) pp. 269–282.
[49] D.A. Yphantis, Biochemistry 3 (1964) 297.
[50] E.T. Adams, Jr. and M.S. Lewis, Biochemistry 7 (1968) 1044.
[51] K.E. Van Holde and R.L. Baldwin, J. Phys. Chem. 62 (1958) 734.
[52] R.V. Webber, J. Amer. Chem. Soc. 78 (1956) 536.
[53] G. Kegeles, S.M. Klainer and W.J. Salem, J. Phys. Chem. 61 (1957) 1286.
[54] H.-G. Elias, Ultrazentrifugen – Methoden, Beckman Instruments, GMBH, Munich (1961) p. 190.
[55] E.T. Adams, Jr., Proc. Nat. Acad. Sci. U.S. 51 (1964) 109.
[56] R.C. Deonier and J.W. Williams, Proc. Nat. Acad. Sci. U.S. 64 (1969) 828.
[57] R.L. Baldwin and J.W. Williams, J. Amer. Chem. Soc. 72 (1950) 4325.
[58] R.L. Baldwin, W.M. Saunders and P.G. Squire, J. Amer. Chem. Soc. 74 (1952) 1542.
[59] J.W. Williams, Fortschr. Chem. Org. Naturstoffe 18 (1960) 434.
[60] R.L. Baldwin and K.E. Van Holde, Fortschr. Hochpolym.-Forsch. 1 (1960) 451.
[61] D.J. DeRossier, P. Munk and D.J. Cox, Anal. Biochem. 50 (1972) 139.
[62] R.M. Carlisle, J.I.H. Patterson and D.E. Roark, Anal. Biochem. 61 (1974) 248.
[63] G.V. Schulz, Z. Physik, Chem. A170 (1944) 168.
[64] J.E. Blair and J.W. Williams, J. Phys. Chem. 68 (1964) 161.
[65] G.R. Anderson, Arkiv för Kemi 20 (1963) 513.
[66] P.F. Fahey, D.W. Kupke and J.W. Beams, Proc. Nat. Acad. Sci. U.S. 63 (1969) 548.
[67] L.H. Peebles, Jr., Molecular Weight Distributions in Polymers (Wiley–Interscience, New York, 1971).
[68] I.H. Billick, M. Schulz and G.H. Weiss, J. Res. Nat. Bur. Stand. 71A (1967) 13.